

The Effect of *namH* Disruption in *Mycobacterium tuberculosis* on the Pathogenesis of Experimental Tuberculosis

Jesse Hansen

Experimental Medicine, McGill University, Montreal

February 2011

A thesis submitted to McGill University in partial fulfillment of the requirements of the
degree of Master of Science (MSc)

© Jesse Hansen 2011

Table of Contents

ABSTRACT	4
ACKNOWLEDGEMENTS	5
1. INTRODUCTION	6
1.1 INNATE IMMUNITY	6
1.2 TUBERCULOSIS	7
1.3 THE MYCOBACTERIAL CELL WALL	8
1.4 NOD2	14
1.5 N-GLYCOLYL MDP	19
1.6 <i>NAMH</i> , N-GLYCOLYL MDP AND <i>M. TUBERCULOSIS</i>	24
2. MATERIALS AND METHODS	25
2.1 BACTERIAL STRAINS, GROWTH CONDITIONS, ELECTROPORATION TECHNIQUES, REAGENTS.....	25
2.2 NUCLEIC ACID TECHNIQUES	25
2.3 MUTANT CONSTRUCTION AND COMPLEMENTATION	26
2.4 LIPID ANALYSIS.....	29
2.5 <i>IN VITRO</i> GROWTH OF <i>MTB. ΔNAMH</i> STRAIN	29
2.6 LYSOZYME AND AMPICILLIN MINIMAL INHIBITORY CONCENTRATION DETERMINATION	30
2.7 PEPTIDOGLYCAN PURIFICATION AND SOLUBILISATION	30
2.8 MICE.....	31
2.9 MOUSE INFECTION STUDIES.....	31
2.10 HISTOPATHOLOGY	33
2.11 FIGURES AND STATISTICS	33
3. RESULTS	34
3.1 <i>NAMH</i> KNOCKOUT	34
3.2 <i>IN VITRO</i> CHARACTERIZATION	34
3.3 AMPICILLIN AND LYSOZYME SUSCEPTIBILITY	36
3.4 HPLC ANALYSIS OF MUROPEPTIDES	38
3.5 LONG-TERM MOUSE INFECTIONS	40
3.6 SHORT-TERM MOUSE INFECTIONS	42
3.7 NOD2-DEFICIENT MOUSE INFECTIONS	44
3.8 RAG-KNOCKOUT MICE STUDY	47

4. DISCUSSION	49
4.1 THE ROLE OF MDP IN IMMUNITY	49
4.2 INFLAMMATORY RESPONSE	50
4.3 PAMPS AND PRRS	52
4.4 AN UNIDENTIFIED RECEPTOR OF <i>N</i>-GLYCOLYL MURAMIC ACID	54
4.5 THE COMPLEMENT STRAIN.....	54
4.6 FUTURE DIRECTIONS	56
4.7 CONCLUSIONS.....	58
<u>REFERENCES.....</u>	<u>59</u>
<u>APPENDICES</u>	<u>70</u>
APPENDIX I: PEPTIDOGLYCAN PURIFICATION AND SOLUBILISATION AND HPLC ANALYSIS	70
APPENDIX II: TABLE OF MOUSE AGE AND GENDER FOR AEROSOL INFECTIONS.....	73

ABSTRACT

Peptidoglycan-derived muramyl dipeptide (MDP) activates the host immune response through the NOD2 receptor. Mycobacteria produce an unusual, glycosylated form of MDP, through the action of the enzyme *N*-acetyl muramic acid hydroxylase (NamH), that is more potent and more efficacious at inducing NOD2-mediated host responses. We set out to test the importance of this modification in *M. tuberculosis* by disrupting the *namH* gene (*Rv3818*). An allelic exchange strategy using a thermosensitive *sacB*-containing vector was used to create *M. tuberculosis* Δ *namH* strain which was confirmed by Southern blot and then complemented with an integrative plasmid. HPLC analysis revealed the *namH* knockout was devoid of *N*-glycolyl muramic acid. *In vitro*, the *namH* knockout had no alteration in either growth kinetics or cellular morphology, while it was mildly more susceptible to ampicillin and no more susceptible to lysozyme compared to the parent strain. *In vivo*, *namH* disruption resulted in increased pathology in the lungs of C57BL/6 mice at early time points, with reduced lymphocytic infiltration to the site of infection. As *namH* disruption did not result in any differences in the bacterial burden, these results suggest that the modified MDP is critical to the immunogenicity of *M. tuberculosis*. To test this, the *namH* knockout was introduced into a mouse devoid of an adaptive immune response, where it led to prolonged survival. Ongoing studies are testing the effect of *namH* disruption in macrophage culture and testing the NOD2-dependence of the *in vivo* phenotype, as well as the long-term survival of DBA2-C57Bl/6 hybrid mice infected with the *namH* knockout strain.

Le muramyl dipeptide (MDP) dérivé de peptidoglycan actionne la réponse immunitaire de l'hôte via le récepteur Nod2. Les mycobactéries produisent une forme inhabituelle de MDP qui est glycosylé, grâce à l'enzyme hydroxylase d'acide muramique N-acétylé (NamH). Cette forme de MDP est plus puissante et plus efficace pour induire une réponse immunitaire de l'hôte via le récepteur Nod2. On a testé l'importance de cette modification dans la *M. tuberculosis* en interrompant le gène *namH* (*Rv3818*). La souche *M. tuberculosis* Δ *namH* a été créée par échange allélique en utilisant un vecteur thermosensible qui contient un *sacB*. Cette modification a en suite été confirmée par un Southern blot puis complémenté avec un plasmide intégratif. Une analyse à l'aide de chromatographie en phase liquide à haute performance (HPLC) a montré que le *namH* knockout n'avait pas d'acide *N*-glycolyl-muramique. *In vitro*, le *namH* knockout n'avait aucun changement dans sa croissance où sa morphologie cellulaire, tandis qu'il été plus susceptible à l'ampicilline et ni plus ou moins susceptible aux lysozymes en comparaison à la souche parentale. *In vivo*, l'interruption du *namH* a mené à une pathologie plus importante des poumons de souris C57BL/6 tôt dans l'infection, et a réduit l'infiltration lymphocytaire après deux semaines d'infection. Aucune différence a été notée dans le nombre d'unités formant des colonies (CFU), ce qui suggère que le MDP modifié est nécessaire à l'immunogénéicité de la *M. tuberculosis*. Le knock-out *namH* a prolongé la survie des souris infectées qui manquent un système immunitaire adaptatif. Des études en-cours testent l'effet de l'interruption du *namH* dans des cultures de macrophages et testent la dépendence-Nod2 de phénotype *in vivo*. Aussi, elles testent la survie à long-terme de souris hybrides DBA2-C57Bl/6 infectées avec la souche knock-out *namH*.

ACKNOWLEDGMENTS.

I thank the members of the Behr, Reed, and Schurr laboratories for their scientific and technical support as well as continuous inspiration. In particular I thank Pilar Domenech for her guidance and encouragement throughout my entire project. I also thank Vlad Kamenski for his invaluable assistance with animal experiments and Fiona McIntosh for her training and advice. I thank Frederic J. Veyrier and Ivo G. Boneca of the Pasteur Institute in Paris, France for their experiments with the cell wall purification and muropeptide analysis. I would like to thank my advisors Michael Reed, Maziar Divangahi, and Danuta Radzioch for their constructive advice and feedback on my project. Most of all I thank my supervisor Marcel Behr for his unlimited patience and excellent guidance without which this project could not have been completed. J.H. was supported by a CIHR Operating Grant (MOP-86536) to Marcel A. Behr.

Part 1: Introduction

1.1: Innate Immunity

In 1989, Charles A. Janeway Jr. put forth a sobering proposal to the scientific community at the Cold Spring Harbour Symposium in New York – that there was an enormous gap in their understanding of the specific adaptive immune system [1]. He explained that “ideas, especially good ideas, can so satisfy our desire to explain what we are studying that they can inhibit our ability to explore” in referring to the domination in thinking regarding the role of humoral immunity in controlling infection. With great prescience, he predicted that the primary detection of highly conserved microbial antigens would be found to be essential for the instruction and mobilization of the secondary adaptive immune response. In his lecture, Janeway referred to Freund’s complete adjuvant (FCA), a mixture containing heat-killed *Mycobacterium tuberculosis*, as the immunologist’s “dirty little secret” that could produce responses of humoral immunity to a variety of antigens when administered in conjunction. By stimulating innate receptors, which he termed pattern recognition receptors (PRRs), the host could discriminate between infectious non-self from non-infectious self [2]. The dependence of humoral immunity on the activation of PRRs by pathogen-specific antigens, which he termed pathogen-associated molecular patterns (PAMPs), allows the system to work coherently and effectively against the invading microbe. He hypothesized about the evolution of such a two-step system, and described how it endowed vertebrates with protection from a nearly infinite variety of pathogens without putting the host at much risk [2,3]. Janeway concluded his talk by explaining that innate receptors, which are able to quickly respond to stimuli and are found in most organisms, not only pre-date clonally distributed receptors, but they directly acted as the foundation for their

evolution. He redirected the field of immunology toward innate immunity and ushered in a new paradigm of immune recognition that persists even today.

As a legacy from Janeway's impressive insight, today it is established that there are a variety of PRRs known to be involved in recognition of microbes, including but not restricted to bacteria. These PRRs can be separated into four main groups: Toll-like receptors (TLRs), C-type lectin receptors (CLRs), nucleotide binding oligomerization domain (NOD) receptors and retinoic acid-inducible gene 1 protein (RIG-1) helicase receptors. TLRs have been implicated in detecting an array of antigens ranging from lipopolysaccharide (LPS) to flagella, CLRs can detect carbohydrate structures, NOD receptors can detect peptidoglycans and RIG-I receptors can detect single or double-stranded RNA from viruses [4]. Each receptor, in its own right, contributes to the elaboration of innate and adaptive immune responses, while genetic defects altering their ability to function properly can lead to devastating diseases [4].

1.2: Tuberculosis

Among the many infectious diseases rampant today, tuberculosis (TB) merits investigation at the level of innate immune recognition for at least two reasons. First, according to the World Health Organization (WHO) TB report 2010, currently about one third of the world's human population is infected with *M. tuberculosis (Mtb)*, which is the worst in South-East Asia, Western Pacific regions, and especially sub-Saharan Africa [5]. For reasons unknown, only about 10% of people infected end up developing active Tuberculosis disease [5]. The problem is further exacerbated in Africa where over 80% of the HIV-positive Tuberculosis-

caused deaths occur. The most recent estimates suggest roughly 1.7 million deaths per year due to Tuberculosis, over three-quarters of which were in HIV-negative cases. Although global prevalence and incidence of active TB is falling, there are an increasing number of drug-resistant and multidrug-resistant *Mtb* (MDR-TB) infections which raises concerns for the future. Thus, there is clearly a need for a better understanding of how our body interacts with the TB bacillus, and interactions with the innate immune receptors seem to be the most logical place to start. The second reason to study innate immune recognition of TB is the long-observed capacity of the TB bacillus to induce innate immune responses. As highlighted in Janeway's lecture, the mycobacterial cell wall confers a notably strong capacity to elaborate a more robust adaptive immune response to unrelated antigens. It follows that a biochemical study of the mycobacterial cell wall will not only point to bacterial PAMPs that interact with the host innate immune system, but potentially hold the key to novel approaches to immunizing against TB itself.

1.3: The Mycobacterial Cell Wall

The structural composition of the mycobacterial cell wall and the contained PAMPs began to be investigated in the 1960s and 70s mainly from a handful of researchers in Japan and France [6-8]. After several decades of dormancy, this field exploded again with advances in technologies such as nuclear magnetic resonance (NMR) imaging and mass spectrometry (MS). Today, our understanding of the mycobacterial cell wall is far from complete, but it is sufficient for studies of biomedical science and basic microbiological investigations. The mycobacterial cell wall contains a highly complex array of proteins, polysaccharides, and lipids that form an exceptionally thick and impenetrable barrier (**Fig. 1**). The innermost component is an

asymmetric plasma membrane bi-layer, of which the outer leaflet is slightly thicker due in part to phosphatidylinositol mannosides (PIMs) [9]. As is explained later, these PIMs may serve as anchorage points for other proteins and polysaccharides. Directly surrounding the plasma membrane is the cell wall core: a covalently linked network of peptidoglycans (PGN), arabinogalactans (AG), and mycolic acids; this core is also sometimes termed the mycolyl-arabinogalactan-peptidoglycan (mAGP) complex. The most common form of PGN found in bacteria consists of repeating units of *N*-acetylglucosamine (GlcNAc) and modified muramic acid (Mur) joined by β -1,4-glycosidic linkages [10]. The adjacent PGN polymers are bound through interactions of the tetrapeptide side-chains on muramic acid which generally extend outwards as follows: *L*-alanyl-*D*-isoglutaminyl-meso-diaminopimelyl-*D*-alanine (*L*-Ala-*D*-Glu-*meso*-DAP-*D*-Ala) [11]; occasionally an additional *D*-alanine may be added to the end to create a pentapeptide [11,12]. The energy required for the cross-linking of the peptides is thought to be derived from cleavage of the terminal *D*-Ala or *meso*-DAP molecules [13]. This general type of PGN is very similar to that observed in mycobacteria, but with three important differences: 1) the *meso*-DAPs are amidated [9], 2) the polypeptides crosslink *via* either two *meso*-DAPs or a *D*-ala and *meso*-DAP in an approximately 1:2 ratio [13], and 3) the 2nd carbon of the muramic acid residue is preferentially *N*-glycolated instead of *N*-acetylated [8,14,15]. It was later discovered that this *N*-glycolated form of muramic acid conferred immunostimulatory properties to the PGN of mycobacterial cell walls [16]. The subject of *N*-glycolation of the muramic acid molecule shall be re-visited later on, as it is the focus of this thesis. Regarding the length of the peptide side-chains, *Mtb* and *M. smegmatis* for example are dominated by tetrapeptides, with some tri-peptides and traces of di-peptides, but this is not necessarily true of all mycobacteria [17]. Directly connected to the muramic acid residue of the PGN is the complex

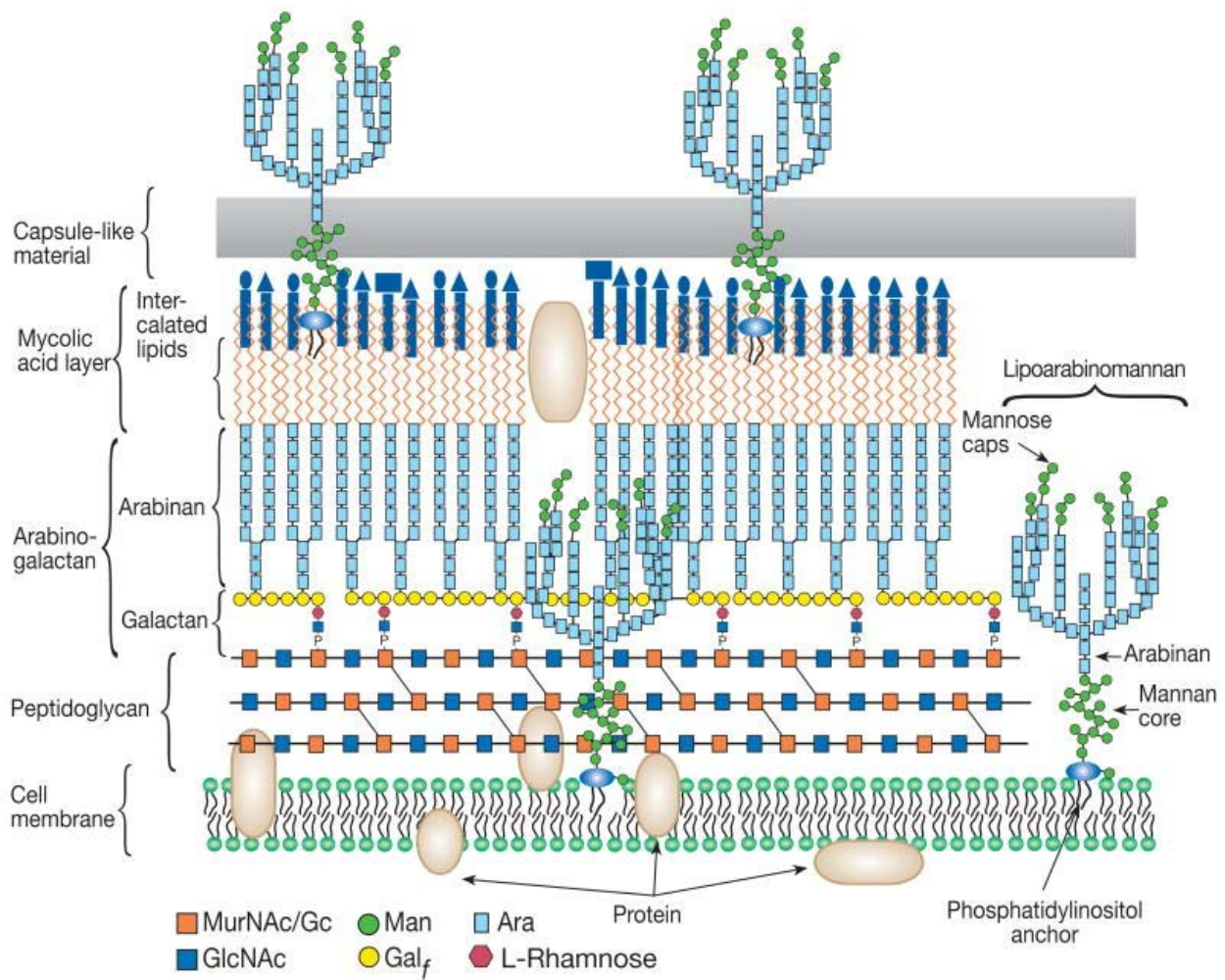


Figure 1. Schematic of the mycobacterial cell wall. Beginning at the bottom, the most interior part of the mycobacterial cell wall is the lipid bi-layer which contains a high proportion of phosphatidylinositol mannosides (PIM) on the outer leaflet. Surrounding the lipid bi-layer is the cell wall core, composed of the peptidoglycan (PGN) layer, the arabinogalactan (AG), and the mycolic acids. The PGN layer is composed of repeating units of *N*-acetylglucosamine and modified muramic acid residues. The long PGN chains are attached to one another through peptide cross-linking bonds between two *meso*-DAPs or a *meso*-DAP and a D-alanine. Through a rhamnose-*N*-acetylglucosamine linker the galactans of the AG layer are attached to the PGN. Covalently attached to the arabinans are the long-chain mycolic acids, which create a nearly impenetrable wall for the cell. Within the hydrophobic zones of the mycolic acids sit a variety of lipids such as trehalose-6,6'-dimycolate (TDM) or lipoarabinomannans (LAM) that confer many virulence attributes to mycobacteria. LAM can be attached to the outer membrane of the lipid bi-layer or can be found in the outer edges of the cell wall. In the capsule, the wax-like structure of the exterior, can be found molecules such as PDIM, which exert strong virulence effects on the host cell. Figure reproduced with permission from Esko et al., 2009.

saccharide network, the arabinogalactan (AG) layer. The galactan (galactofuranose sugars) portion of the AG is joined by an essential rhamnose-*N*-acetylglucosamine linker to the 6th carbon of the muramic acid residue in the PGN [18] and the arabinan chains are then attached to the 5th carbon of these galactofuranose residues [19]. These AG cell wall components have long been known to be one of the main serologically active polysaccharides of the cell wall [16,20]. The mycolic acids are the most exterior component of the mycobacterial mAGP core, and they are attached through the 5th carbon of the arabinose residues in the AG [21]. The impermeability of the mycobacterial cell wall is likely attributable to these long chain fatty acids (70-90 Carbons) that tend to pack tightly together [9].

Intercalated in the deep hydrophobic regions of the mycolic acids can be found a variety of free lipids: phthiocerol dimycocerosate (DIM/PDIM), trehalose-6,6'-dimycolate (TDM; also called cord factor), sulfolipids (SLs), phenolic glycolipids (PGL), PIMs, lipoarabinomannans (LAM), trehalose-based lipooligosaccharides (LOS), and others [9,22]. These lipids, combined with mycolic acids, make up about 60% of the mycobacterial cell wall and can be readily extracted *in vitro* using hydrophobic solvents, allowing for individual study and characterization. There are at least three exemplary extractable free lipids that have been well studied and characterized: Cord factor, LAM, and the PDIMs. Cord factor has been shown to exert severe toxicity in mouse models, even in small doses (10µg) it can be lethal; strangely, in high doses (>50µg) it is rarely lethal [22]. Cord factor has been shown to increase cytokine (Tumour necrosis factor- α (TNF- α) and interleukin-6 (IL-6), for example) secretion in macrophages, and has also been shown to be able to inhibit phagosome-lysosome fusion [23]. Recently, it has been shown by two groups that Cord factor is recognized by the host receptor Mincle (macrophage inducible C-type lectin) [24,25]. LAM molecules either sit in the outer lipid layer of the cell

wall or are attached at the cell membrane through PIMs, but in either case they are presented on the exterior of the cell [26]. LAM from *Mtb* has been shown to inhibit T-cell proliferation and to alter bactericidal functions of macrophages by abrogating interferon- γ (INF- γ)-mediated MHC class II antigen presentation and reducing the number of toxic free oxygen radicals [27]. The terminal branches in many strains of virulent and non-virulent mycobacterial are sometimes capped with mannosyl residues, creating mannosylated LAM (ManLAM) [26]. There is some evidence of different degrees of mannosylation in LAM that is apparently more associated with bacterial growth than linked to a virulence phenotype [26,28,29]. It has been observed for example that *M. bovis* Bacillus Calmette-Guerin (BCG) [28] and *Mtb* Erdman strain [30] have 40-70% of their LAM mannosylated, but *M. smegmatis* is devoid of this modification [31]. There is also an interesting observation that non-mannosylated LAM is about 100 times more potent at eliciting TNF- α responses [32], and is also a strong inducer of INF γ [33] and IL-12 [34]. The ManLAM binding is mediated through the host mannose receptor in macrophages, which has also been shown to be capable of inducing phagocytosis [35]. In addition, Man-LAM has been shown to bind and enter dendritic cells (DCs) largely through the DC-specific intercellular adhesion molecule-3 grabbing non-integrin (DC-Sign) [36]. Once again, the mannosylation of the LAM seemed to play an important role in this function, as the slow growing *Mtb* and *M. bovis* BCG were better able to exploit DC-Sign compared to the faster-growing *M. smegmatis* [37]. The pathogenic *Mtb* appears to misuse the DC-Sign receptor to reduce the functionality of TLRs (particularly TLR4) and to induce IL-10 expression [38]. Thus, Man-LAM in *Mtb* may serve to regulate entry into the host cell, as well as survival once within. Finally, PDIMs are a waxy structure of the outer lipid layer (otherwise known as the “capsule”) and are important for full virulence of *Mtb* in mice [39,40]. PDIM apparently works as a

virulence factor by modifying the acute phase of interactions between the host cell and bacterium. For example, it has been shown to help mediate interplay between *Mtb* and *M. bovis* BCG at the host plasma membrane in a cholesterol-dependent fashion that permits entry into the cell [41]. This may be partly due to the re-localization of cholesterol-enriched lipid rafts moving to the site of pathogen-membrane interaction in order to mediate phagocytosis [42,43]. Consequently, PDIM-deficient strains of *Mtb* are less able to infect macrophages [41]. Furthermore, once inside the cell, phagosomes containing PDIM-deficient *Mtb* acidify more quickly, yet apparently does not alter phago-lysosome fusion [41,44]. It is also noteworthy that PDIM-deficient *Mtb* elicit more inflammatory cytokines such as TNF- α and IL-6, but not IL12-p40, from murine macrophages and dendritic cells [44]. To date, a receptor for PDIM has not been identified. Interestingly, in spite of the aforementioned observations, the growth and survival of PDIM-deficient strains of *Mtb* within resting macrophages was unaltered [41,44]. However, when infecting activated macrophages, the growth of the PDIM-deficient strain was attenuated due to an increased susceptibility to nitric oxide-dependent killing [44]. It was recently shown that PDIM can be spontaneously lost through routine *in vitro* passaging, and thus it is an important quality-control measure to continuously check laboratory strains for this lipid, especially when working with virulent strains [45]. In summary regarding the overall structure of the mycobacterial cell wall, although in general it is the mAGP complex that is considered essential for the viability of mycobacteria, it is usually the outer soluble lipid portion that is considered essential for virulence and disease [22]. This does not imply, however, that there do not exist indirect effects of the mAGP in virulence and disease. The complexity and diversity of the mycobacterial cell wall has certainly contributed to the remarkable persistence of this genus

throughout evolution, and it is only through understanding the nature and dynamics of its constituents will we be able to control the diseases that mycobacteria cause.

1.4: NOD2

As Charles Janeway insightfully envisioned the immense control that PRRs assert over adaptive immunity and host survival, today we know of a wide variety of these receptors that are capable of sensing almost any kind of conserved structure on an invading microbe. Among them are the intracellular nucleotide oligomerization domain (NOD) leucine-rich-repeat containing receptors (NLRs) which are specific for cytosolic antigens. There exist two known NOD receptors – NOD1/CARD4 and NOD2/CARD15 – which can detect PGN from gram negative [46,47] or gram positive [48,49] bacteria. Unlike NOD1, which is expressed in virtually every adult tissue [50,51], NOD2 expression is restricted to monocytes, macrophages, dendritic cells, and certain specialized epithelial cells [52,53]. Both receptors are similar in structure, containing one (NOD1) or two (NOD2) N-terminal caspase recruitment domains (CARD), a centrally-located nucleotide-binding domain (NBD), and a C-terminal regulatory domain consisting of 10 leucine rich repeats (LRRs) [50,51,53]. The CARD domain appears to be the most biologically active part of the NOD proteins, as it is the minimal functional unit required to elicit nuclear factor- κ B (NF- κ B) activation. Although these domains are similar in sequence to apoptosis-regulating domains, they do not *per se* induce apoptosis, but they have been shown to enhance apoptosis induced by caspase-9 expression [48,51,53,54].

Upon activation, NOD2 receptors undergo a conformational change and oligomerize *via* their NBDs which promotes CARD-CARD interaction with Receptor interacting protein-2 (RIP2) [53,55], a serine/threonine kinase that is then able activate the NF- κ B pathway [56]. Mechanistically, RIP2 accomplishes this through the ubiquitination of the NF- κ B modulator NEMO [57]. In addition to RIP2 activating the NF- κ B pathway, which is typically involved in the transcription of pro-inflammatory response genes [55], it activates the c-Jun N-terminal kinase (JNK) [58], a member of the mitogen-activated protein kinase (MAPK) family that further activates an adaptive immune response [59]. The LRR apparently has a role in the negative regulation of the CARD domain, as its deletion in NOD2 resulted in a five-fold up-regulation of NF- κ B [53]. Experimental evidence suggests the LRR region serves an auto-inhibitory role which is relieved upon conformational changes induced by the NOD2 ligands [52]. Interestingly, these LRRs have been proposed to serve as sensors of bacterial LPS [60], but this function in NOD2 remains to be demonstrated in a biological system other than HEK293 cells transfected with NOD2-expressing plasmids [48,61,62]. Moreover, these studies may present a very serious risk of LPS contamination by PGN which could create an apparent NOD2-dependent LPS response. In fact, there is an abundance of studies in primary murine macrophages or human dendritic cells (DCs) and peripheral blood mononuclear cells (PBMCs) demonstrating that the detection of LPS is NOD2-independent [63-67].

NOD2 has been identified as a non-redundant mycobacterial recognition receptor of peptidoglycans that can induce cytokine responses in monocytes [68]; NOD1 showed a much more modest response when comparing *Mtb* sonicates [68]. To be more precise, NOD1 receptors have been demonstrated to be specific for the D-Glu-*meso*-DAP portion of the muramic acid peptide side chains [47] while NOD2 receptors have been demonstrated to be

specific for the muramyl dipeptide (MDP), i.e. muramic acid and the proximal L-Ala–D-Glu residues, component of PGN [49,69]. It is also worth mentioning that there seems to be a synergistic effect between TLRs and NOD2 that may be observed depending on the cell type and experimental conditions. It has been demonstrated in murine cells, for example, that LPS activation can induce NOD2 mRNA expression [70], or that MDP-mediated activation can increase MyD88 expression, which in turn may cause increased sensitivity to TLR responses [71]. Furthermore, both NOD2 and TLR pathways seem to converge on RIP2, and RIP2-deficient mice show defects in TLR and NOD2-mediated signalling [72]. The complex interactions between these receptors suggests that they have evolved to potentiate one another in order to maximize responses to invading microbes, and indeed it seems reasonable that such a system exists for NOD2.

Polymorphisms in *NOD2* have been associated with a number of human diseases, including TB [73], Leprosy (Hansen's disease) [74], Blau syndrome [75] and Crohn's disease [61,76,77]. Given that different polymorphisms have been linked with different diseases, it is important to determine the location and nature of these polymorphisms in order to better understand the phenotypic effect, if any, on protein function. The association of NOD2 polymorphisms is best established in Crohn's disease, a condition previously labelled as autoimmune [78], but for which functional analysis of NOD2 is pointing to a new model of disease pathogenesis. This *3020insC* NOD2 mutation associated with Crohn's disease is in the extreme C-terminus end, truncating the tenth leucine repeat [61,77], which is precisely the region believed to be involved in MDP recognition [54]. The NOD2fs mutation produces a protein that is unable to respond to its peptidoglycan ligands, yet is still functional in the CARD domain and can induce NFκB upon over-expression [49,61]. Supporting this prediction, mononuclear cells

(MNCs) from patients with a Crohn's disease-associated polymorphism, the *3020insC* frameshift mutation (NOD2fs), secreted 65% to 80% less TNF- α compared to heterozygotes or wild-type controls when stimulated with *Mtb* [68]. Indeed this interesting *Mtb* PAMP detection defect associated with a Crohn's disease susceptibility polymorphism has galvanized several hypotheses about the possible involvement of other mycobacteria, specifically *Mycobacterium paratuberculosis*, in the chronic inflammation observed in the intestinal tract of Crohn's disease patients [79]. Indeed it may seem paradoxical that a loss-of-function mutation in a receptor that normally instigates a host immune response can lead to a disease defined largely by excessive inflammation, and the mechanisms of the disease resulting from loss-of-function NOD2 mutations are not well understood. One study showed that the NOD2fs also apparently lessens IL-10 secretion, an anti-inflammatory cytokine and positive regulator of suppressor T cells [66], while others have proposed that this defect in NOD2 leads to diminished commensal microbiota handling in the gut due to blunted α -defensin and cryptidin which consequently leads to persistent inflammation [80-82]. There is also some evidence that commensal microbiota positively regulate NOD2, which creates a negative feedback loop to regulate the bacteria in a mutual balance of symbiosis [82]. Although these are not entirely satisfactory explanations, they highlight the complexity of such a NOD2 mutation in human disease. It should also be noted here that the multiple other CD-associated NOD2 polymorphisms have also been shown to result in decreased PGN recognition [54]. In Blau syndrome (BS), a second granulomatous disorder associated with NOD2 polymorphisms, all of the mutations seem to be localized to the NBD [75,83]. It is interesting to note the difference in phenotype compared to the Crohn's disease mutation in the LRR, as these BS-associated mutations were shown to have increased basal levels of NF κ B activity [84].

As a direct consequence of the above observations regarding NOD2 mutations in human disease, there have been a rapidly increasing number of studies in the last decade looking at the functionality of NOD2 knockouts or knock-downs in the mouse model. For example, due to the role of NOD2 in pathogen recognition, mice that lack the NOD2 receptor succumb earlier than wild-type controls when infected with *Mtb* [64]. Immunological studies of these *Nod2*^{-/-} mice showed an overall trend of defective innate and adaptive immune responses to mycobacterial infection: mice had reduced production of type I cytokines measured in bronchoalveolar lavage (BAL) fluid as well as in *ex vivo* infections, and reduced CD4⁺ and CD8⁺ T cell recruitment [64]. In addition, when the authors assayed *Mtb* infection in these mice there was consistently less pathology observed in the lungs of *Nod2*^{-/-} mice despite similar bacterial burdens at 4 and 8 weeks post-infection; it should also be noted that the bacterial burden was mildly (but statistically significant) higher in the lungs of *Nod2*^{-/-} mice at 24 weeks post-infection. These, and other [85-87], experiments clearly demonstrate an important role of NOD2 in handling a variety of bacterial infections not only through innate mechanisms of defence but also through the instruction of the adaptive immune system. More recently, the function of DC cross-presentation has been explored [88], where administration of MDP plus antigen significantly enhanced cross-presentation of CD8⁺ T cells, as well as increasing expression of DC co-stimulatory molecules. At a minimum, this study secured an important role for DCs in NOD2-dependent host responses. Thus NOD2 may serve as a canonical innate receptor that Charles A. Janeway Jr. was referring to.

The NOD2 receptor also apparently plays a perhaps unexpected role in the induction of autophagy [89], an ancient system of eliminating damaged or mis-folded proteins and in coping

with intracellular pathogens [90,91]. This NF- κ B-independent process was demonstrated to be NOD2-dependent in dendritic cells [92], macrophages [93], and colon epithelial cells [94] by treatment with the NOD2-agonist MDP. One possible function of the autophagic response is that it may serve to deliver cytosolic antigens to MHC class II receptors for presentation and subsequent adaptive immune instruction [92]. Two of the above three publications have shown NOD2-mediated autophagy to be RIP2-dependent [92,94] while the third proposed a RIP2-independent process [93]. Given the aforementioned CARD-CARD interaction between NOD2 and RIP2, it seems likely that the process should be RIP2-dependent. Briefly, NOD2 seems to promote the recruitment of ATG16L1 (autophagy related 16-like 1) to the site of bacterial entry [93], encapsulating the bacteria, and meanwhile this in turn may create a positive feedback loop for MDP-induced NOD2 signalling [94]. Finally, it has also been demonstrated that several CD-associated NOD2 variants are less capable of initiating autophagy in response to MDP [92,94]. This NOD2-autophagy link may certainly help shed light on the current understanding of Crohn's disease aetiology, as the genes most reproducibly associated with Crohn's disease are *NOD2* and the autophagy genes, *ATG16L1* and *IRGM* [95,96].

1.5: *N*-glycolyl MDP

As previously mentioned, there is a unique structural modification to the muramic acid residue in the PGN of mycobacterial cell walls – the carbon 2 is preferentially *N*-glycolated rather than *N*-acetylated (**Fig. 2A**). This simple addition of a hydroxyl group can have profound consequences on PGN immunogenicity and is therefore the subject of increasing research efforts today. The biosynthesis of the *N*-glycolated muramic acid residue has been recognized for over

30 years [97], as well as the inclusion of radio-labelled atmospheric oxygen into the glycolyl group [98] and energy from NADPH [99]. The pathway basically proceeds as follows: UDP-*N*-GlcNAc → UDP-MurNAc → UDP-MurNGly before being incorporated into the PGN [7]. In other words, the hydroxylation reaction takes place on the last soluble cytoplasmic UDP-MurNAc-pentapeptide precursor before being transported across the plasma membrane for integration into the PGN [12,99]. This *N*-glycolyl modification seems to be made on about 70% of the muramic acid residues of the PGN in some mycobacteria studied such as *Mtb* [100] or *M. smegmatis* [101], leaving the remaining 30% in the *N*-acetylated form. Interestingly, *N*-glycolation of carbohydrates appears to be very rarely used in nature, and when they are used they seem to confer differential biological activities to those specialized molecules [102]. Notably, these PGN modifications have been observed in several other closely related genera also containing mycolic acids such as *Rhodococcus*, *Tsukamurella*, *Gordonia*, *Nocardia*, *Skermania*, and *Dietzia* [14,103,104]. The only genus so far discovered that contains mycolic acids but not *N*-glycolated MDP is *Corynebacterium* [14]. Furthermore, there is another group of closely related genera that do not contain mycolic acids but have *N*-glycolyl modified PGN: *Actinoplanes*, *Asanoa*, *Catellatospora*, *Catenuloplanes*, *Couchioplanes*, *Dactylosporangium*, *Glycomyces*, *Longispora*, *Microbacterium*, *Micromonospora*, *Okibacterium*, *Pilimelia*, *Spirilliplanes*, *Verrucosispora*, and *Virgisporangium* [99]. All of the aforementioned genera, as well as that of *Mycobacteria*, are part of the class of *Actinomycetales* [105], and indeed in bacterial taxonomy the *N*-glycolyl modification can be used as a classification criterion for *Actinomycetales* [106].

The existence of a unique muramic acid *N*-glycolyl modification within a particular subset and class of bacteria implies the existence of a hydroxylation enzyme encoded within their

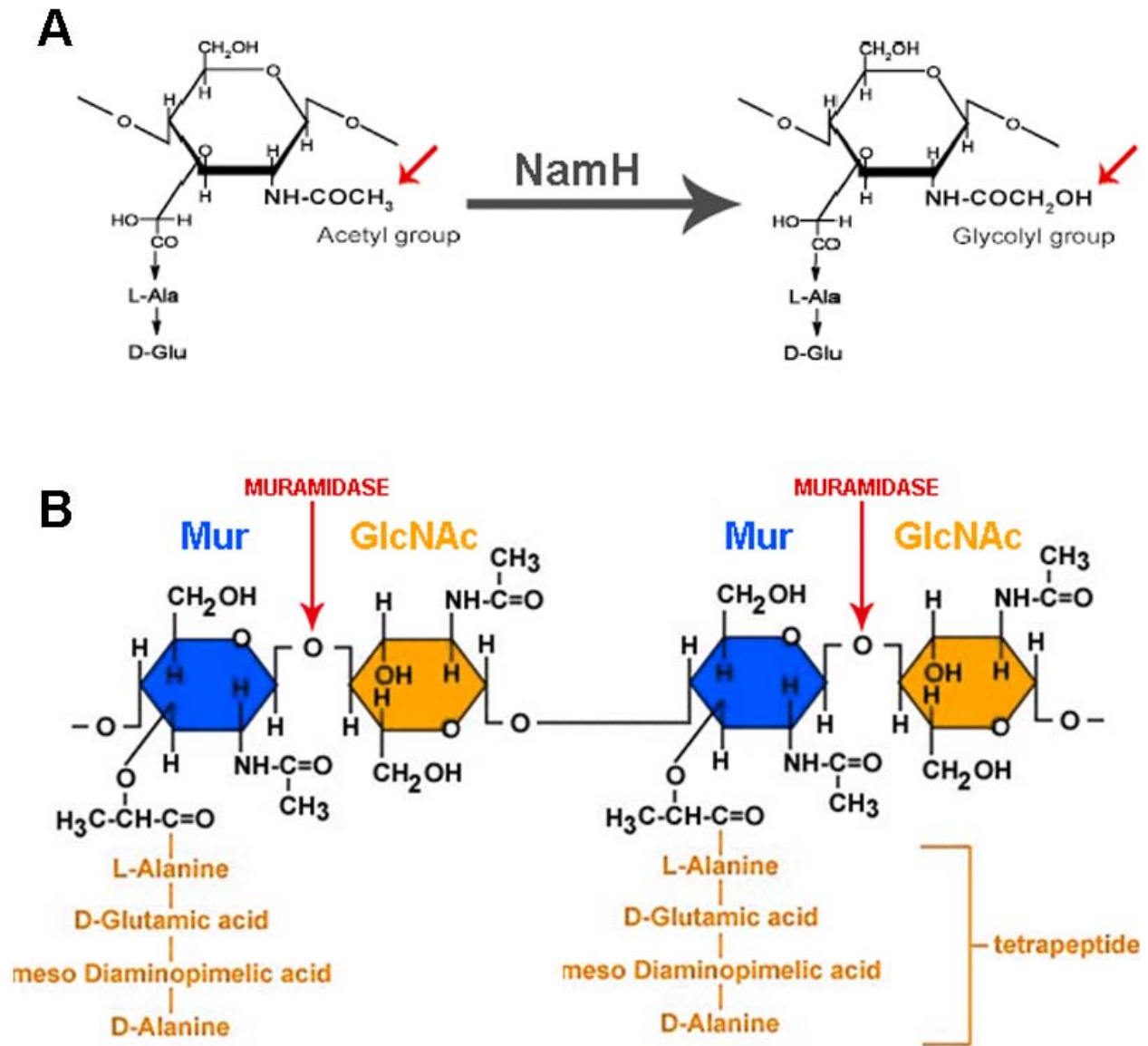


Figure 2. NamH hydroxylation of MDP and PGN hydrolysis by lysozyme. (A) The muramyl dipeptide (MDP) molecules that comprise one of the two alternating units of the PGN are one of many muramic acid molecules with varying peptide side-chain lengths. The acetyl group at carbon 2 is commonly acetylated in bacteria, but through the action of the NamH enzyme this group is modified to be glycolated (red arrows). In most organisms the reaction is incomplete, leaving a small proportion of *N*-acetyl MDP molecules. Figure reproduced with permission from Coulombe et al., 2009. (B) Muramidase (also known as lysozyme or mutanolysin) cleaves bacterial PGN at the linkages of adjacent muramic acids (Mur) and *N*-acetylglucosamine (GlcNAc) liberating disaccharides. This schema shows the more commonly found tetra-peptide side-chain, which is the dominant form in Mycobacteria. Note here that the carbon 2 is acetylated rather than glycolated, as it is this acetylated form that is thought to be the best substrate for muramidase cleavage.

genomes. With this knowledge, Raymond and colleagues did a BLAST search for the murine CMP-*N*-acetylneuraminic acid hydroxylase (responsible for the *N*-glycolation of sialic acids), the only other muramic acid hydroxylase enzyme known to exist, and identified a homolog (Rv3818) in the *Mtb* H37Rv genome [101]. Upon knockout of this gene in *M. smegmatis*, the authors showed abolition of *N*-glycosylated PGN precursors and thus Rv3818 was then called *N*-acetyl muramic acid hydroxylase (NamH). Interestingly, this enzyme was also found to be present and functional across all of the aforementioned organisms for which *N*-glycosyl modifications have been described [101], with the exception of *M. leprae* which has a pseudogene copy of *namH* [107] and consequently makes only *N*-acetylated PGN [17]. Initial studies of the *namH* knockout strain in *M. smegmatis* attempted to demonstrate a susceptibility to β -lactam antibiotics and lysozyme, a muramidase that cleaves the PGN backbone (**Fig. 2B**), but were only able to reveal subtle phenotypes on the order of one dilution difference in susceptibility to both agents [101]. These experiments were driven by the hypothesis that the hydroxyl group contained within the *N*-glycosyl moiety conferred additional hydrogen bonding, and therefore stability, within the cell envelope [9,101]. In interpreting their results, they reasoned that the *N*-acetylated PGN precursors could affect peptide side-chain cross-linking, weakening the PGN, and were therefore more susceptible to β -lactam antibiotics. Furthermore, they reasoned that the function of the *N*-glycosyl group was to protect cleavage of the β -1,4 PGN linkages from lysozyme. Interestingly, when lysozyme susceptibility experiments were repeated in nutrient-rich media there was over a log-fold increase in susceptibility of the *namH* mutant strain; the authors did not offer an explanation for this finding. A study looking at the genetic elements that have been conserved or deleted in 100 different *Mtb* clinical isolates revealed that *namH* was intact in all cases [108], while a genome-wide study of *Mtb* did not expose *namH* as

an essential gene required for either optimal growth [109,110], or survival within the macrophage [111]. The evidence for the non-essential nature of NamH is further strengthened by the fact that it can be knocked out in *M. smegmatis* without any obvious change in viability *in vitro* [63,101]. These observations seem to imply a selective pressure to maintain *namH* for an as-of-yet un-identified role in persistence within the host. Indeed, the function of NamH in the virulence and persistence of *Mtb* within the host is previously un-addressed.

Given the immunomodulatory properties of MDP [112,113] and the exquisite responsiveness of NOD2 to MDP [49,69], the *namH*-dependent *N*-glycolation modification in a NOD2-dependent fashion was addressed. Studies of purified ligands showed not only that *N*-acetyl MDP detection was dependent on NOD2 [49], but that *N*-glycolyl MDP had an even greater immunostimulatory effect that was also NOD2-dependent [63]. It was also demonstrated that macrophages from *Nod2*^{+/+} mice secreted more TNF- α upon infection with wild-type *M. smegmatis* when compared to *namH*-deficient *M. smegmatis*, which was not the case in *Nod2*^{-/-} mice [63]. The amount of TNF- α secretion did not vary depending on NOD2 status when infected with the *namH*-deficient *M. smegmatis* strain, which likely reflected the ability of additional cell wall components to stimulate an immune response [63]. The authors also demonstrated that during *in vivo* infection the host was less responsive in terms of cytokine secretion, in a NOD2-dependent fashion, to the *namH*-deficient *M. smegmatis* strain. The studies clearly demonstrated the immunogenic properties of the conversion product *N*-glycolyl MDP which, in the context of the entire organism, was abrogated in the absence of NOD2.

1.6: *NamH*, *N*-glycolyl MDP and *M. tuberculosis*

With this knowledge in mind, we set out to disrupt *namH* in *M. tuberculosis* in order to study the effects of reduced immunogenicity of the PGN layer on the pathogenesis of infection by *M. tuberculosis*. By selectively disrupting the *namH* gene we were able to modify the PGN in a way that allowed us to study the function of the *N*-glycolyl modification in a pathogenic mycobacterial species that has co-evolved with humans for millennia, but throughout this time, retained this unusual modification that favours host immune recognition. We hypothesized that the reduced immunogenicity of the *MtbΔnamH* strain would result in an organism less well detected by the host, thereby permitting it to replicate and spread within the host in a manner comparable to what was observed when *NOD2*-knockout mice were infected with *Mtb*. According to this hypothesis, *MtbΔnamH* might ultimately result in a reduced survival time of infected mice, and increased bacterial burden in the lungs with concomitantly reduced pathological phenotypes. In other words, we hypothesized that *NOD2* is an evolved receptor specifically for the relatively recent *N*-glycolyl modification in mycobacteria, and therefore removing the *N*-glycolyl group would allow the invading microbe to better evade the host immune responses.

Part 2: Materials and Methods

2.1: Bacterial Strains, Growth Conditions, Electroporation Techniques, and Reagents

The stock of *M. tuberculosis* H37Rv was derived from a strain originally obtained from the Pasteur Institute (Paris, France), thus known as H37Rv-Pasteur. All strains of *M. tuberculosis* were grown at 37°C in Middlebrook 7H9 medium (Difco laboratories) supplemented with 10% albumin-dextrose-catalase (ADC) (BD biosciences), 0.05% tween 80 (Sigma-Aldrich) and 0.2% glycerol, or on 7H11 agar (Difco laboratories) supplemented with 10% oleic acid-supplemented ADC (OADC) (BD biosciences). Hygromycin B (50µg/ml) (Multicell), kanamycin monosulphate (25µg/ml) (Multicell), or 2% sucrose (Sigma-Aldrich) was added where indicated. Electrocompetent *M. tuberculosis* was prepared and electroporated as previously described [114]. For plasmid DNA cloning, the ElectroMAX DH5α-E competent *Escherichia coli* cells (Invitrogen) were used. All *E. coli* was grown in Luria-Bertani (LB) broth or on LB agar (BD Biosciences) with hygromycin (200µg/ml) or gentamicin (5µg/ml) (Multicell) where indicated.

2.2: Nucleic Acid Techniques

Mycobacterial DNA was extracted as previously described [115] and Southern blot and hybridization technique performed as previously described [116]. For confirmation of gene knockout by Southern blot, genomic DNA was digested with *Cla*I overnight and transferred to a Hybond-N nylon membrane (Amersham Biosciences) where it was hybridized with a 1.8kbp PCR amplicon probe of the *namH* gene.

2.3: Mutant Construction and Complementation

Gene knockout of *namH* was accomplished by a two-step allelic-exchange strategy using a thermosensitive-*sacB* replicative vector as previously described [115]. Briefly, a 210bp fragment in the 5' region of the *namH* gene was replaced by a hygromycin-resistance cassette. A 2327bp fragment containing the whole *namH* gene plus 750bp upstream (**Fig. 3A**) was PCR amplified using the following primers: NamH-B (5'-GGACTAGTTGCAGCACGATCCAGCTGTAC-3') and NamH-F (5'-CGACTAGTTTGCCGTCGGCAGGCCGGT-3') and cloned into the pcDNA2.1 (Invitrogen) vector at *SpeI* restriction fragment sites using the pcDNA2.1-containing ampicillin-resistance cassette for selection on LB agar. This plasmid was called pJH1, and several clones containing this plasmid were sequenced in order to ensure there were no mutations in *namH* flanking genes. The 1534bp hygromycin-resistance cassette was then inserted into the *namH* gene using the restriction enzymes *BstBI* and *NdeI* and selected on hygromycin-containing LB agar, and the plasmid was called pJH2. Finally, the ends of the *namH::hyg* fragment were blunted after excision and inserted into the mycobacterial shuttle vector pPR23 using the restriction enzyme *SpeI* and selected for using the pPR23-containing gentamicin-resistance cassette on LB agar, and the finalized plasmid was called pJH3 (**Fig. 3B**). This plasmid was then sequenced at the 5' and 3' ends to ensure correct insertion into the plasmid, as well as to be sure there were no mutations in the *namH* flanking genes. The pJH3 plasmid containing the disrupted *namH* gene was electroporated into *M. tuberculosis* strain H37Rv Pasteur and plated on 7H11 with 50µg/ml hygromycin at 32°C for 5 weeks. Colonies were then picked and grown in 10ml of 7H9 with

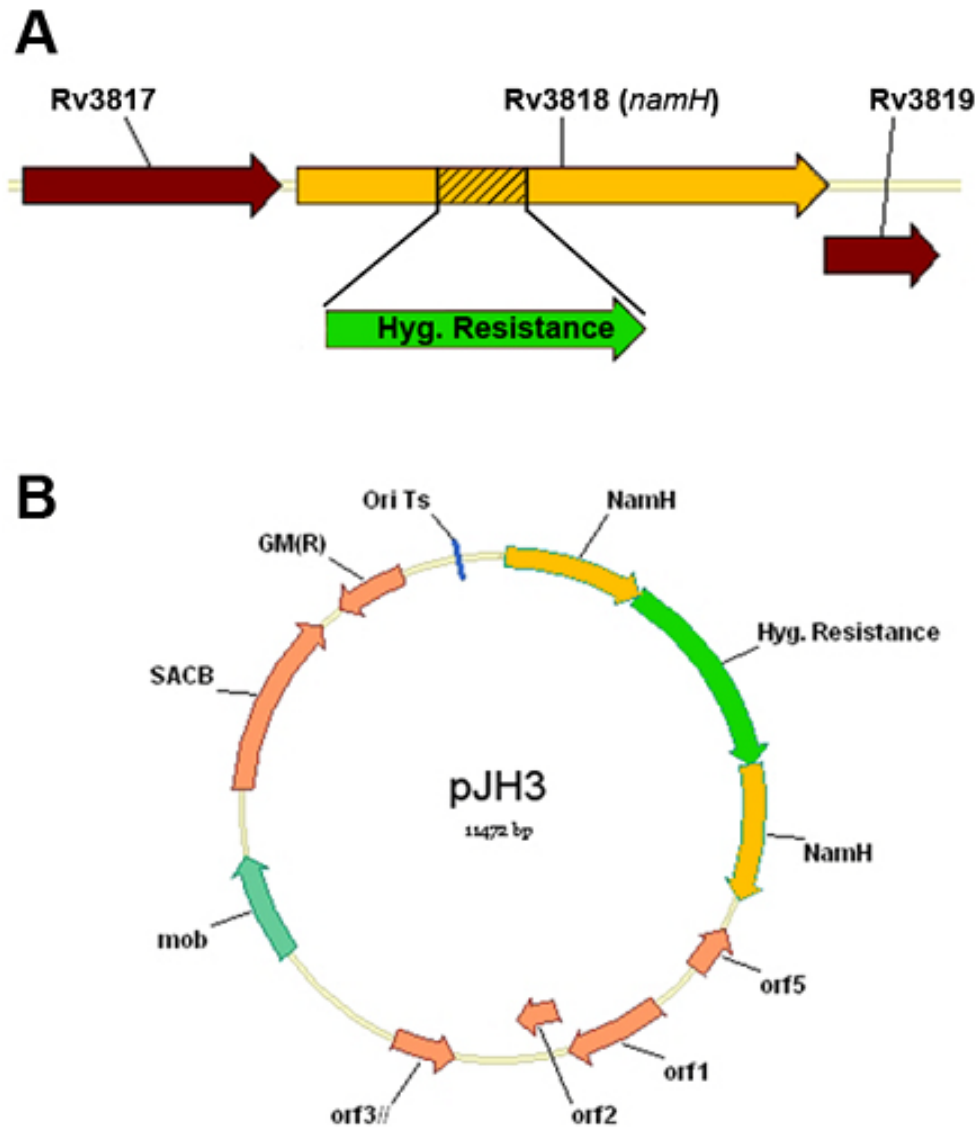


Figure 3. Schematic of the *namH* gene and the construct used for targeted knockout. (A) Genetic region showing *namH* (Rv3818) and surrounding genes. A 2.3kbp fragment containing the *namH* gene and upstream regions were PCR amplified and disrupted using a hygromycin-resistance (Hyg^{R}) cassette. A 200bp region in the 5' region of the gene was excised where the Hyg^{R} cassette was inserted in order to further ensure genetic disruption. (B) pJH3 is the plasmid construct used to knockout *namH*. The above-mentioned Hyg^{R} cassette-disrupted *namH* gene was cloned into pPR23 shuttle vector containing a temperature-sensitive origin of replication (Ori Ts), a gentamicin selection cassette (GM(R)), and a *sacB* gene which confers sucrose sensitivity in mycobacteria. The *sacB* gene and temperature-sensitive origin of replication permitted the two-step allelic exchange to accomplish genetic disruption of *namH*.

50µg/ml hygromycin at 32°C until being plated 1-2 weeks later on 7H11 with 50µg/ml hygromycin and 2% sucrose with incubation at 39°C for 3-4 weeks, permitting the selection of *namH* double-crossover mutants. Resulting colonies (resistant to hygromycin, sucrose, and the non-permissive temperature of 39°C; Hyg^R Suc^R T^R) were expanded in 7H9 with 50µg/ml hygromycin and were confirmed to have a disrupted genomic copy of *namH* by PCR amplifications and Southern blot.

The mutants were complemented with the *namH* gene under either the native or the *hsp60* promoters. The native complement plasmid was produced by PCR amplification using a high fidelity Platinum Pfx polymerase (Invitrogen) of an 1854bp region containing the *namH* gene (including the 292bp upstream region containing the native promoter) using the following primers: MTNamHF (5'-TCACCCAACACCAT-3') and MTNamHR (5'-ACAACGCCGTCGTC-3'). The amplicon was then inserted into the mycobacterial integrative vector pMV306 using the restriction enzymes *Hind*III and *Nhe*I (for the insert), and *Hind*III and *Xba*I (for the vector). The *hsp60*-driven *namH* plasmid was produced by PCR amplification of a *namH* fragment that started at the first in-frame codon of the 5' end of the gene using the following primers: NamHG (5'-GTGCAGGTCACAAGCGTTGGT-3') and MTOPNamHR (5'-TGCATCATGGCCGTG-3'). This amplicon was then cloned into pMV261 using the restriction enzymes *Bam*HI (blunted) and *Hpa*I (for the insert) and *Mls*I (for the vector) where it was positioned so that the *hsp60* promoter was directly adjacent to the 5' end of *namH*. The insert orientation was confirmed by PCR. The *hsp60::namH* fragment was then excised and inserted into pMV306 using *Xba*I and *Hind*III. Complementation plasmids were sequence-confirmed to be mutation-free for *namH*. Both complementations were confirmed by extracting DNA of the

recipient *Mtb* and performing PCR amplification of the kanamycin-resistance cassette contained within pMV306.

2.4: Lipid Analysis

Apolar lipid extraction and analysis was performed following an adapted protocol from Slayden & Barry 2001 [117], as previously described [45]. 100µl aliquots of log-phase growth cultures was added to 1ml 7H9 containing 0.1µCi of sodium 1-C¹⁴ propionic acid (specific activity 54 mCi/mmol) (American Radiolabeled Chemicals) and incubated with continuous rolling for one week at 37°C. The culture was then centrifuged and the pellet re-suspended in 600µl methanol:0.3% *aq.* NaCl (10:1, v/v) and 300µl petroleum ether was subsequently added. After 10 min of vigorous shaking, the samples were spun for 10 min at 15,000g, and supernatants (containing the apolar lipids) were recovered and dried under an air current. Samples were re-suspended and vortexed in 25µl petroleum ether. 10µl of each sample were spotted onto 250µm Silica Gel 60 TLC plates (EM Science) and run 3 times in a system of Petroleum Ether and Ethyl acetate in a ratio of 98:2, v/v. After drying, TLC plates were visualized using a Storm 840 PhosphorImager (GE Healthcare).

2.5: *In vitro* Growth of *Mtb*Δ*namH* Strain

For the *in vitro* growth curves of all strains, bacterial cultures were grown to mid-exponential phase and adjusted to an OD₆₀₀ of 0.1, diluted 1:100 in 7H9 in a final volume of 50ml and allowed to grow for 13 days at 37°C with constant rolling. OD₆₀₀ measurements and

plating for CFU was done every 2 to 3 days. On days 8, 11, and 13 the cultures were diluted 1:4 and later multiplied by a factor of 4 in order to obtain the undiluted OD₆₀₀ value.

2.6: Lysozyme and Ampicillin Minimal Inhibitory Concentration Determination

For lysozyme and ampicillin susceptibility assays, bacterial cultures were grown and adjusted to an OD₆₀₀ of 0.1 as described above, then diluted 1:100 in 7H9. Using a multi-channel pipette, 100µl of culture was added to four rows per strain of a 96-well plate containing sequential two-fold dilutions of ampicillin (100µg/ml → 0.05 µg/ml) or lysozyme (5mg/ml → 0.002mg/ml) and incubated at 37°C. After 14 days, the MIC was determined to be the minimum concentration required to fully inhibit visible growth within the wells and averaged between the four replicates.

2.7: Peptidoglycan Purification and Solubilisation

M. tuberculosis strains were grown in a 500ml volume of standard glycerol-supplemented 7H9 growth medium, with or without the addition of antibiotics where necessary. Cultures at OD₆₀₀ 0.6-0.8 were centrifuged at 4°C and re-suspended in 10ml ice-cold H₂O to prevent PGN degradation. The bacilli were then added, drop by drop, to 10ml of sterile 8% SDS warmed to 100°C. Samples were autoclaved at 121°C for 60 mins in order to safely be exported from the containment-level 3 (CL-3) facility. Samples were then sent to the Pasteur Institute in Paris, France, where F. J. Veyrier and I. G. Boneca continued the purification process. For a complete description of their protocol see **Appendix 1**.

2.8: Mice

$Nod2^{+/-}$ males backcrossed onto a C57BL/6 background were obtained from the Congenics Facility at Yale University. These mice were bred with C57BL/6 mice purchased from Harlan Laboratories to establish a $Nod2^{-/-}$ breeding colony at the McGill University Health Centre. A wild-type breeding colony was established from the $Nod2^{+/+}$ progeny and were used as wild-type controls for the aerosol infection involving $Nod2^{-/-}$ mice. A comprehensive list of the heterogeneous age and gender of the mice used in aerosol studies making use of $Nod2^{-/-}$ mice and their controls is attached as **appendix 2**. These mice were used for the data in **figure 7b**. The C57BL/6 mice used for **figure 7a** were all 6-8 week old females (The Jackson Laboratory), as were the $Rag1^{-/-}$ mice that lack an adaptive immune system (B6.129S7- $Rag1^{tm1Mom}/J$; developed on a C57Bl/6J background) (The Jackson Laboratory) used for the survival study. The mice used in the long-term survival study were 8-10 week old female hybrids between DBA2/2J and C57BL/6J mice (B6D2F1/J) (The Jackson Laboratory) that are known to be slightly more susceptible to *Mtb* infection [118]. All experiments were conducted in accordance with the guidelines and regulations of the animal research ethics board of McGill University.

2.9: Mouse Infection Studies

Prior to aerosol infections, cultures were grown to an OD_{600} of 0.5 and stored as 10% glycerol stocks at -80°C . Quantification of glycerol stocks was performed by plating serial dilutions onto 7H11 plates. CFU were counted after 3-4 weeks of incubation at 37°C . Inocula

were prepared by diluting these stock cultures 1/40 (H37Rv WT and H37Rv Δ *namH* complement under the native promoter) or 1/100 (H37Rv Δ *namH*) in PBS/Tween (0.05%). 7-8 week old C57Bl/6 mice (Jackson) and Rag1^{-/-} mice were aerosolized for 10 min using a Lovelace nebulizer (model 01-100, In Tox Products). Five mice were sacrificed 24 hours after infection and both lungs were homogenized, diluted, and plated in order to determine CFU present in each mouse. The respective numbers for each strain were: 34 CFU (H37Rv WT), 51 CFU (H37Rv Δ *namH*), and 97 CFU (H37Rv Δ *namH* complement). Mice were sacrificed at 3, 6, and 12 weeks after infection for processing lungs and spleen. The left (larger) lung was put in 10% neutral-buffered formalin for histopathologic analysis, and the right (smaller) lung and spleen were homogenized, serial diluted, and plated for CFU analysis. The above experiment was modified and replicated, with the addition of time points at 1, 2, and 18 weeks after infection as well as the inclusion of *Nod2*^{-/-} mice for analysis at 3, 6, and 12 weeks. Corresponding starting bacterial burden for the second aerosol infection were 37 CFU (H37Rv WT), 34 CFU (H37Rv Δ *namH*), and 35 CFU (H37Rv Δ *namH* complement). All mice were processed as described above. The mouse long-term outcome study was performed using 6-8 week old B6D2/F1 mice (Jackson); five C57Bl/6 mice were included in this infection for determination of bacterial burden at day 1 after infection, as described above. The corresponding CFU for that aerosolization were: 39 CFU (H37Rv WT), 20 CFU (H37Rv Δ *namH*), and 33 CFU (H37Rv Δ *namH* complement). Mice were weighed weekly and were compassionately sacrificed if a veterinarian deemed them to be unhealthy/suffering, or if they lost more than 15% of their maximum body weight. Upon sacrifice, lungs were harvested and kept in 10% neutral-buffered formalin for histopathologic verification of cause of death.

2.10: Histopathology

Immediately following mouse sacrifice, the larger (left) lung was put in 10% neutral-buffered formalin and left to expose for at least 24 hours before being sent for processing (Histology Core Facility, Goodman cancer center, McGill University). Tissue was embedded in paraffin and sections 4 to 5 μm thick were processed with standard hematoxylin and eosin (H&E) stains. Slides were evaluated based on overall pathology (atelectasis, pneumonitis) and granuloma formation.

2.11: Figures and Statistics

Survival data was assigned P-values based on the log-rank test. Significant differences in CFU were analyzed using the unpaired t test. For statistics involving CFU in mouse lungs and spleen, standard errors of the mean (SEM) were calculated using 5 mice per group and were deemed significant if $p < 0.05$. Figures were generated using GraphPad Prism version 4.0b (GraphPad Software, San Diego, CA).

Part 3: Results

3.1: *namH* Knockout

Genetic knockout of the *namH* gene was accomplished using a two-step allelic exchange system involving a temperature-sensitive plasmid containing the sucrose-sensitizing gene *sacB* and *namH* disrupted with a hygromycin resistance cassette (**Fig. 3B**). Through sucrose and temperature counter-selection, we generated H37Rv Δ *namH* Pasteur strain. Successful disruption of *namH* was preliminarily tested by PCR across the insertion junctions and subsequently confirmed by Southern blot using a probe specific for *namH* (**Fig. 4A**). Multiple independent isolates of the confirmed-*namH* knockout strain were expanded in broth and tested for PDIM loss, as this has been shown to occur spontaneously during *in vitro* growth (Domenech 2009). Approximately half of the *namH* mutants were negative for PDIM and were discarded, and the remaining strains were kept for further analysis (**Fig. 4B**). To complement the *namH* knockout strain with the endogenous copy of the gene we transformed using two different integrative plasmids containing kanamycin-resistant cassettes, one with the gene under its native promoter and the other under the *hsp60* promoter in order to over-express NamH. All transformants were selected on kanamycin and tested by PCR to confirm that they did not represent spontaneous antibiotic-resistant mutants.

3.2: *In vitro* Characterization

As a first step to understanding the biological effect of the *namH* knockout on *Mtb*, we looked for any differences compared to the wild-type strain and sought to confirm some of the

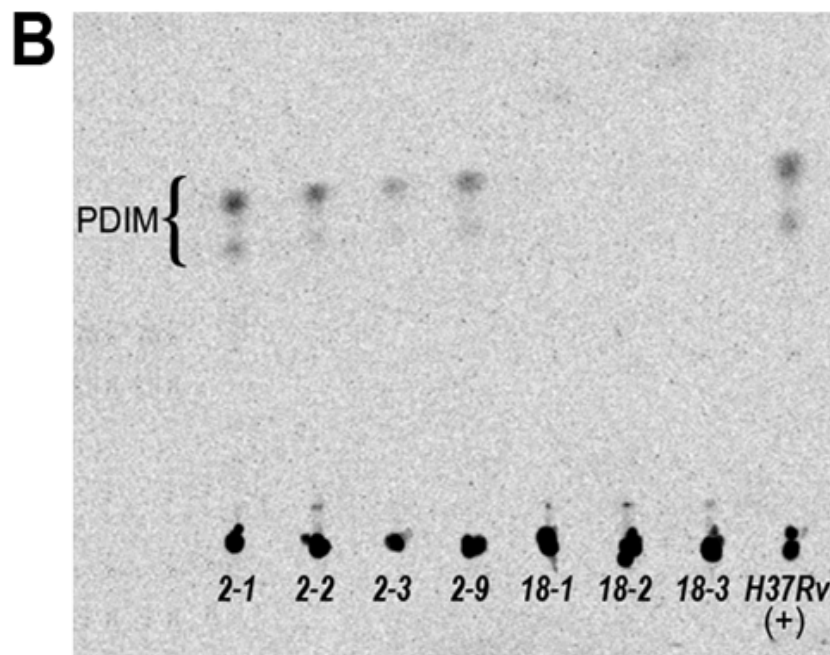
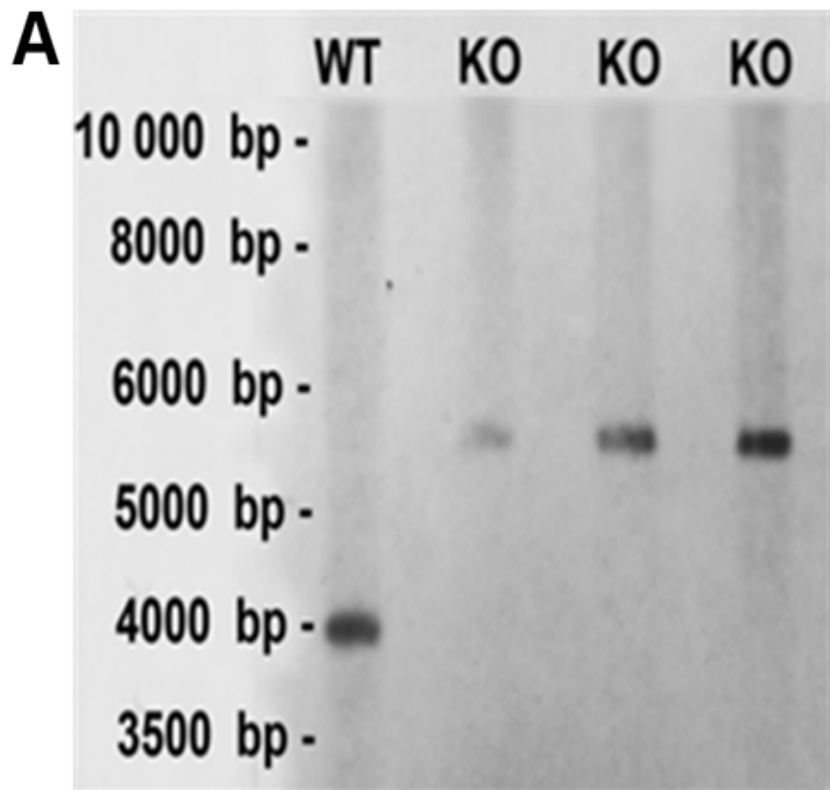


Figure 4. Southern Blot *namH* knockout strain and TLC confirming PDIM. (A) Southern blot showing disruption of *namH* in *Mtb*. DNA from the parent strain H37Rv Pasteur (WT) and three independently isolated *namH* mutants were cleaved with *ClaI* and probed using a 1.8 kbp probe spanning the *namH* region. The band at 4kbp represents the fragment containing the native *namH* gene from the wild-type strain, and the 5.5kbp band represents the same fragment with a hygromycin-resistance cassette inserted in the 5' region of *namH* in order to disrupt it. All three clones were successful *namH* knockouts. (B) PDIM analysis of 7 *namH* knockout isolates (derived from 2 early selection clones). All strains derived from isolate 2 (2-1,2-2,2-3,2-9) were confirmed PDIM positive, and those derived from isolate 18 (18-1,18-2,18-3) were PDIM negative. H37RV (+) is a positive control of a known PDIM-positive strain.

phenotypes observed in the *namH* mutant of *M. smegmatis* [63,101]. We first looked for any difference in *in vitro* growth rate of the *namH* mutant and complements in liquid medium over 13 days. There was no difference between any of the 4 strains in culture density as measured by OD₆₀₀ readings throughout the duration of this experiment (**Fig. 5A**). We observed a puzzling and somewhat consistent trend with the *namH* mutant strain that for a given OD₆₀₀ value, particularly at mid-log growth range, there would be 3 to 4 times as many colony forming units (CFU) on solid medium as compared to the wild-type strain. Since this observation was extremely variable, it was not possible to demonstrate this effect with consistency; nonetheless we were able to take this into consideration for subsequent assays. The mechanism of this discrepancy between OD₆₀₀ and CFU values was never ascertained - perhaps it is a change in optical lucidity or culture clumping. To test for the latter possibility, as well as to assay bacillus morphology, we performed a Ziehl-Neelsen (ZN) stain (**Fig. 5C**). We observed no discernable difference in the *namH* mutant strain, and although clumping was evident in all samples, it did not appear to be particularly worse in the mutant. In addition, the appearance of the individual CFU grown on solid media did not show any obvious differences in shape or size (**Fig. 5B**). Thus, the *namH* knockout appeared to be fully viable and exhibited no differences in growth or morphology when tested *in vitro*.

3.3: Ampicillin and Lysozyme Susceptibility

The minimal inhibitory concentrations (MIC) of ampicillin and lysozyme in the *namH* knockout strain were investigated in order to reproduce a previously-observed susceptibility phenotype of the *namH* mutant in *M. smegmatis* [101]. We were not able to reproducibly show

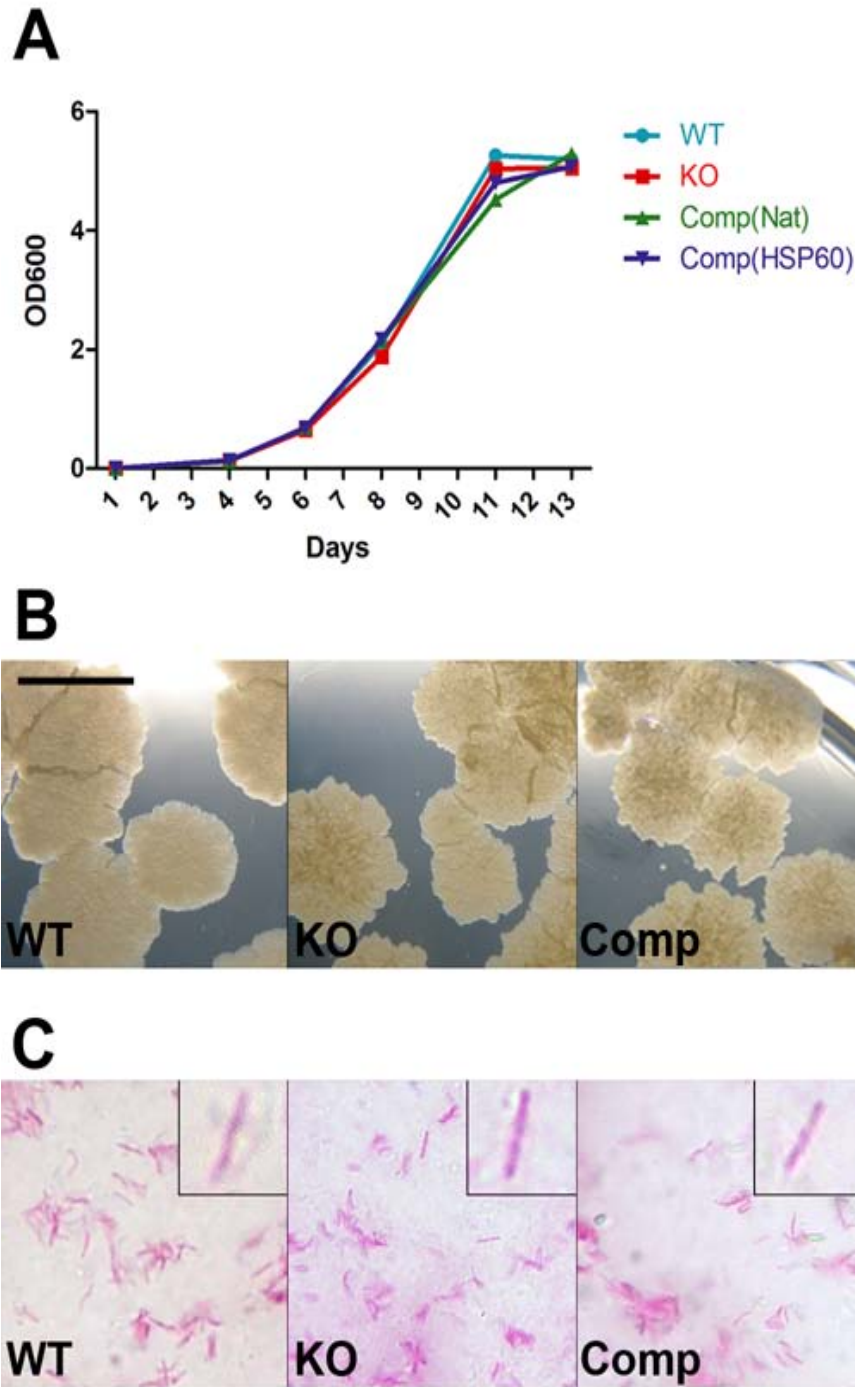


Figure 5. Disruption of *namH* does not alter growth kinetics or morphology *in vitro*. (A) Growth curve of four strains of *M. tuberculosis*: wild type (WT), $\Delta namH$ (KO), and complements under either the native (nat) or *hsp60* (HSP60) promoters. There is no change in growth kinetics between any of the strains when grown in Middlebrook 7H9 liquid medium at 37°C with constant rolling. Results are representative of two independent experiments (B) Colony forming units (CFU) of cultures grown on solid Middlebrook 7H11 agar medium grown at 37°C for 4 weeks. Comp strain is the gene complemented under the native promoter. No obvious differences in CFU morphology were observed. Scale bar, 1cm. (C) Ziehl-Neelsen acid-fast stain of the strains mentioned above magnified 1000X. Insets show a single bacterium of each strain. There appear to be no differences in size, shape, or uptake of stain between the three strains.

any difference in susceptibility to lysozyme, although this may in part be due to the lability of the enzyme [101]. On the other hand, we were able to show a slight increase in susceptibility to the β -lactam antibiotic ampicillin. The approximate estimation of the MIC for ampicillin is 75 μ g/ml for the wild-type strain and 20 μ g/ml for the *namH* knockout strain, representing an approximate 3 to 4 fold increase in susceptibility in the mutant. The MICs obtained in these assays varied frequently between repeat studies, which were further exaggerated by the above-mentioned OD₆₀₀/CFU discrepancy in the mutant strain. The ampicillin-susceptibility assay served as a quality-control measure to verify a phenotype of successful *namH* knockout, and to that end we were able to demonstrate a mildly increased susceptibility to ampicillin.

3.4: HPLC Analysis of Muropeptides

In order to conclusively verify the knockout of *namH* in our strain we performed a direct analysis of the glycolated and acetylated muropeptide molecules in the PGN. We digested and processed cell walls from all four strains of *Mtb* – WT, KO, the complement under the native promoter (Comp(Nat)), and the complement under the *hsp60* promoter (Comp(*hsp60*)) – and subjected them to HPLC analysis (**Fig. 6**). Hydrolysis of *N*-glycolylmuramic acid-*N*-acetylglucosamine links in the PGN by muramidase (also called lysozyme) lead to the liberation of muropeptides composed of disaccharide units (*N*-acetylglucosamine-*N*-glycolylmuramic acid) with varying peptide side-chains attached to the muramic moieties. These peptide side-chains are extremely complex in Mycobacteria as some amino acids may be amidated [9]. It is therefore not surprising that we obtained a complex chromatogram.

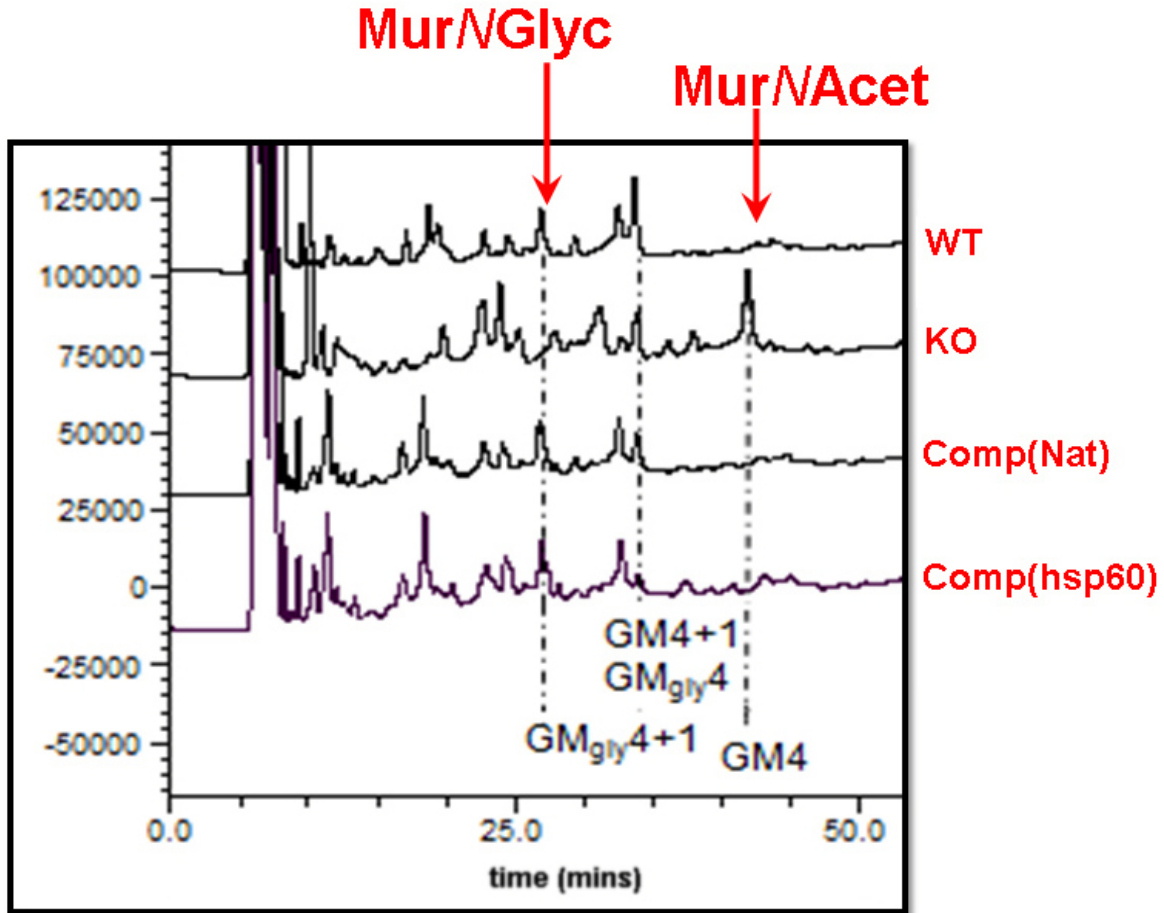


Figure 6. HPLC analysis of muuropeptides from *M. tuberculosis*. Analysis shows *N*-glycolyl muramic acid (MurNGly) and *N*-acetyl muramic acid (MurNAcet) obtained from the PGN of the following strains: H37Rv *wild-type* (WT), *namH* *knockout strain* (KO), and the complement under either the native (nat) or *hsp60* (*hsp60*) promoter. Hydrolysis of *N*-glycolylmuramic acid (Mur) and *N*-acetylglucosamine (GlcNAc) links in the PGN by muramidase lead to the liberation of disaccharide muropetides (GM; G is GlcNAc and M is Mur) with varying peptide side-chain lengths ('4' refers to the tetra-peptide form). Mycobacterial peptide side-chains can be very complex, and the resultant chromatogram is therefore inherently difficult to interpret. Nevertheless, we were able to identify several peaks corresponding to the MurNGly and MurNAcet by mass spec in the *M. smegmatis* samples processed identically. With an identical pattern in *Mtb*, we were able to identify several pairs of muramic acid peaks where the acetylated form would elute approximately eight minutes before the glycolated form. We observed that the WT strain had a mixture of both MurNGly (M_{gly}) and MurNAcet (M) with the former predominating, and that the peaks for *N*-glycolyl muramic acid were entirely eliminated in the *namH* knockout strain, while the peaks for *N*-acetyl muramic acid were markedly increased. Importantly, the peaks in both complement strains returned to the normal chromatogram pattern observed in the WT strain.

Both complemented strains presented a profile similar to that of the wild-type H37Rv strain of *M. tuberculosis*, indicating we had restored *namH* activity in these strains. Therefore, the *namH* knockout strain is devoid of the *N*-glycolylated muramic acid modification and the complement strains have an *N*-glycolyl to *N*-acetyl muramic acid ratio similar to the parent strain.

3.5: Long-term Mouse Infections

In order to study the *in vivo* effect of the *namH* deletion we aerosol infected C57Bl/6 mice, a relatively resistant strain of mice, with three strains of *Mtb*: H37Rv wild-type, *namH* knockout (KO), and the native complement strain (Comp). Aerosol method was chosen because it is the natural route of *Mtb* transmission, and furthermore we chose to infect with a realistically small dose of live bacteria (under 100 CFU per mouse) as is thought to occur in humans. Compared to the infectious dose of around 10^2 bacteria, there is an approximately 4 log₁₀ increase in the first 3 weeks, consistent with what has been described by many groups using the murine model to study aerosolized TB [64,119]. After that point, i.e. between 3 and 12 weeks post-infection, H37Rv numbers did not change in the lungs, while in the spleen there was a relatively constant increase in bacteria (**Fig. 7A**). Analysis of bacterial burden at 3 and 6 weeks post-infection showed no difference between the three strains in the lungs. Interestingly, at 12 weeks there was an approximate 0.9 log fold significant decrease ($p < 0.0001$) in bacterial burden in the lungs of mice infected with the *namH* knockout strain. Unfortunately, the wild-type phenotype was not recovered at 12 weeks in the complement strain, a finding that is perhaps due to the assay variability (both technical and biological) in the samples obtained at this analysis point. Dissemination, as measured by spleen bacterial count, was similar between all three

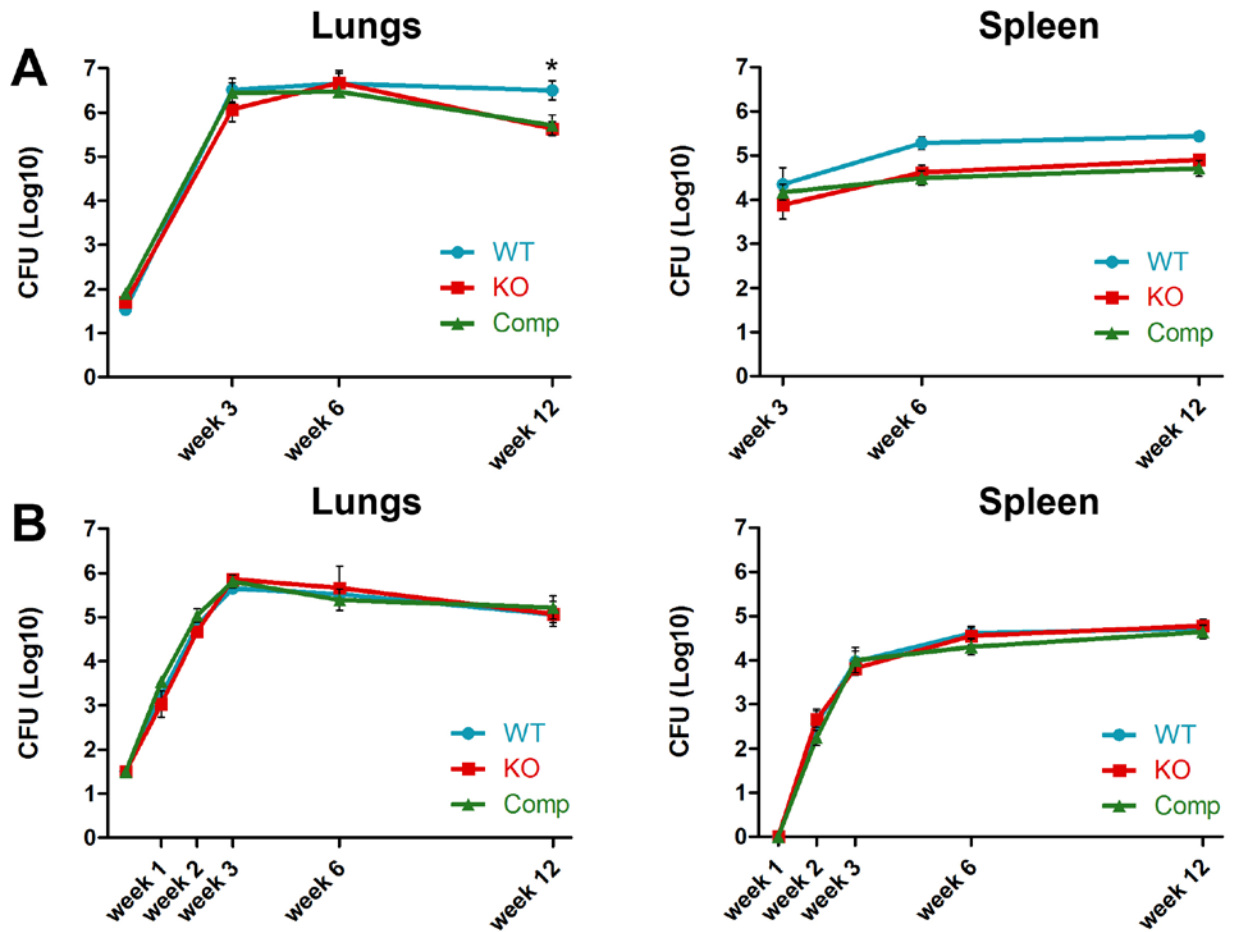


Figure 7. *Mtb* bacterial burden in mouse lungs and spleen. (A) C57Bl/6 mice were aerosol infected with <100 CFU of the following strains of *Mtb*: wild-type H37Rv (WT), *namH* knockout strain (KO), and the complement under the native promoter (Comp). CFU rose rapidly in the first 3 weeks post-infection and slowed thereafter in all strains. At 12 weeks there was a 0.9 log-fold decrease in CFU in the lungs of mice infected with the *namH* knockout strain, which was similar in the complement strain. CFU in the spleen were identical at 3 weeks post-infection, but CFU were significantly lower in the *namH* knockout and complement strains at both 6 and 12 weeks post-infection. (B) In a replicate experiment, C57Bl/6 mice of varying ages were aerosol infected as described above, except with 30-40 CFU for all strains. Bacterial numbers rose rapidly in the lungs during the first 2-3 weeks of infection in all strains, and growth was halted between 3-6 weeks post-infection. After a one week lag-period, bacterial numbers in the spleen rose rapidly for two weeks for all strains and numbers continued to rise slowly between 3 and 6 weeks post-infection. There were no significant differences in lung CFU between any of the three strains tested during the first 6 weeks of study. In contrast to the first infection, we did not observe any difference in splenic CFU at any time point between the strains. 5 mice were used per group. Error bars represent \pm standard errors of the means (SEMs), and an asterisk indicated $P < 0.005$.

strains at 3 weeks post-infection but increased by about 0.6 log at 6 ($p < 0.0003$) and 0.5 log at 12 weeks ($p < 0.001$) post-infection for the H37Rv strain. This is perhaps a reflection of the reduced ability of the *namH* mutant strain to disseminate to the spleen, but it is not known why the complement strain did not revert to a wild-type phenotype (but did recover wild-type phenotype in all other assays) leading us to believe this observation is due to either technical/biological variation or an unusually high bacterial count in the spleens of the mice infected with H37Rv WT at 6 and 12 weeks.

3.6: Short-term Mouse Infections

In order to replicate the findings from the long-term mouse experiment, as well as add two more time points at one and two-weeks post-infection, we performed another aerosol study similar to the previous one, emphasizing earlier time-points. Bacterial numbers rose exponentially for the first two weeks following infection and peaked at 3 weeks (**Fig. 7B**). All three strains grew equally well in the lungs of the mice over the first three weeks of infection, and all disseminated to the spleen equally well. After an initial lag period of 1-2 weeks, bacterial numbers in the spleen quickly began to rise until approximately 3 weeks post-infection where the dissemination began to slow. By six weeks post-infection all strains had been contained by the host adaptive immune response in the lungs and were no longer rising in number. Therefore no changes in CFU were observed over the 6 week period in the *namH* knockout strain or complement. Histopathological analysis of the lungs revealed very little atelectasis or lymphocytic infiltration in the lungs of any of the mice one week post-infection (**Fig. 8**). Unexpectedly, at two weeks the *namH* mutant strain showed a more severe phenotype,

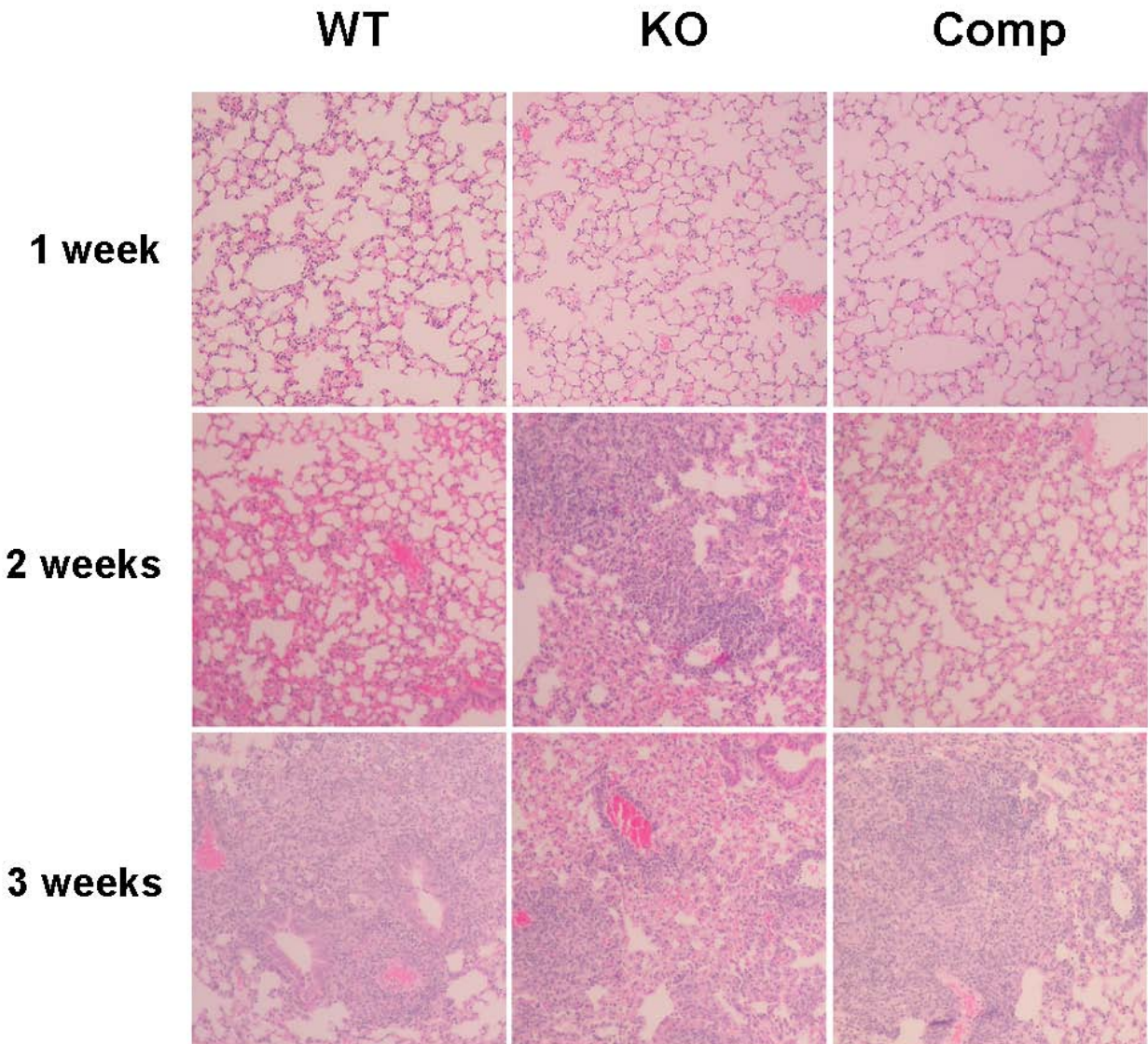


Figure 8. Histopathology of lungs infected with *Mtb*. Hematoxylin and eosin (H&E) stain of mouse lung sections infected with the following strains of *Mtb*: *wild-type* H37Rv (WT), the *namH* knockout (KO), and the complement under the native promoter. Lung pathology was examined in order to qualitatively describe any differences in lymphocyte recruitment or overall lung pathology. At one week post-infection we observed no evident pathology or lymphocyte recruitment in any of the strains tested, and lungs appeared healthy. At two weeks post-infection, we observed a diffuse neutrophilic pneumonitis (strongly pink staining regions) in approximately 80% of the lung as well as diffuse lymphocytic infiltrates (purple regions) and few open airways. In contrast, the lungs of both the WT and complement-infected mice were healthy in appearance with few granulomas. Lungs at three weeks post-infection showed persistent diffuse neutrophilic pneumonitis in the KO strain and large poorly-defined granulomas. The WT and complement strains showed large well-defined granulomas interspersed between regions of healthy-looking tissue. Magnification is 100x.

presenting with large areas of diffuse granulomatous pathology, as evidenced by strongly staining eosinophilic cells in the region. Furthermore, the lungs of these mice were independently ranked by two blinded readers to have the lowest percent of airways intact and the most severe overall pathology of the three strains. The wild-type and complement strains showed mild lymphocytic infiltration with few clearly defined granulomas and mild atelectasis. At three weeks post-infection there was persistent diffuse neutrophilic pneumonitis in the lungs of mice infected with the *namH* knockout strain. This appeared to significantly limit the number of free airways in these mice, and again they were ranked by blinded readers to have the overall worst pathology. Furthermore, there were large granulomatous regions in the *namH* knockout-infected mice that were not clearly defined and generally appeared less well-contained than granulomas observed in the other strains. The wild-type and complement strains appeared to have multiple well-defined granulomas interspersed by large regions of healthy airway. Pathological analysis of 6 weeks was not possible due to excessive variability and more samples have been submitted for analysis; this is an ongoing study that also contains future time points at 12 and 18 weeks post-infection.

3.7: NOD2-deficient mouse infections

In order to study the role of *namH* in the context of a NOD2-deficient host, we included *Nod2*^{-/-} mice in the above aerosol infection study. In agreement with previously studies [64], H37Rv was able to grow equally well in the lungs and spleens of mice at 3 and 6 weeks post-infection similar to the *Nod2*^{+/+} mice (**Fig. 9**). The *namH* knockout strain did not differ in

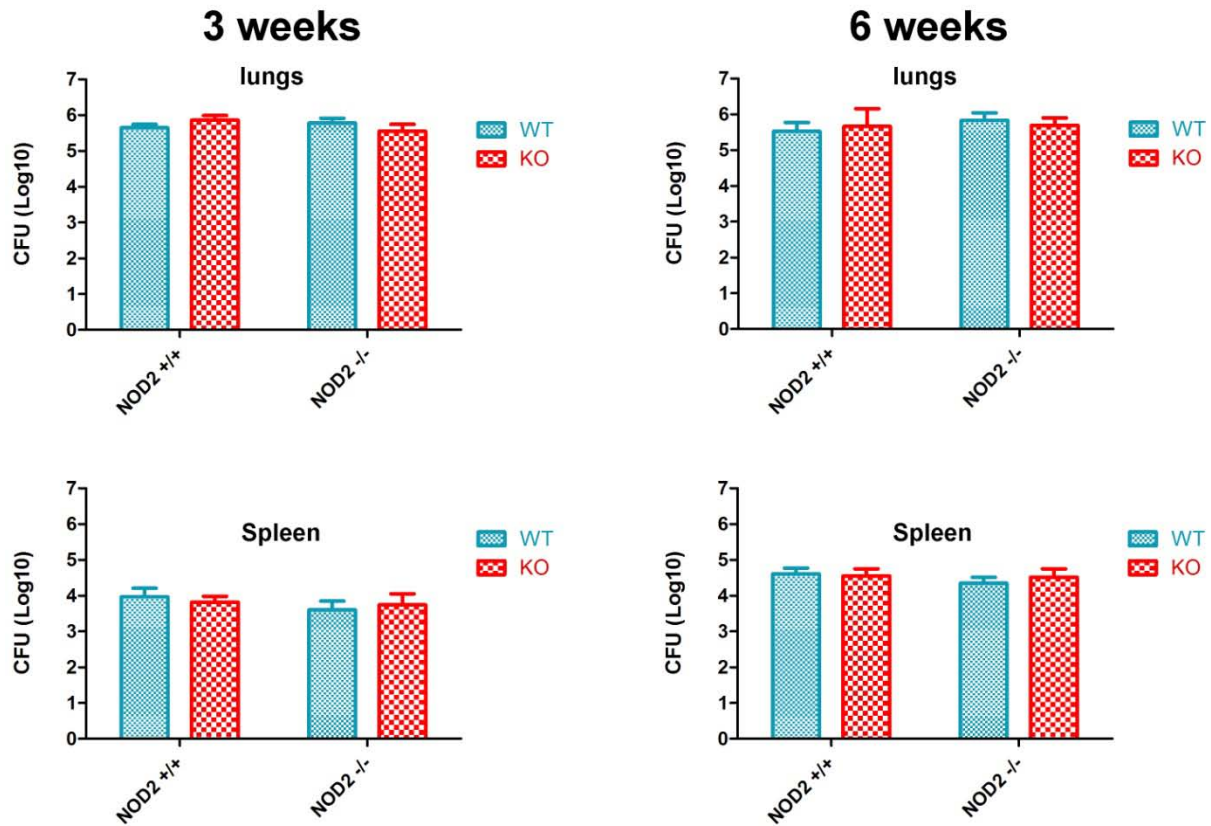


Figure 9. Bacterial burden in the lungs and spleen of NOD2-deficient Mice infected with *Mtb*. *Nod2*^{-/-} mice and their control littermates were aerosolized with 30-40 CFU of virulent H37Rv wild-type (WT) or *namH* mutant strain (KO). Bacterial burdens were measured at 3 and 6 weeks post-infection in the lungs and spleen. At both time points, there was no significant difference found dependent on either *Nod2* status in the mice or *namH* status in *M. tuberculosis*. Five mice were used per group. Error bars represent standard errors of the means (SEM).

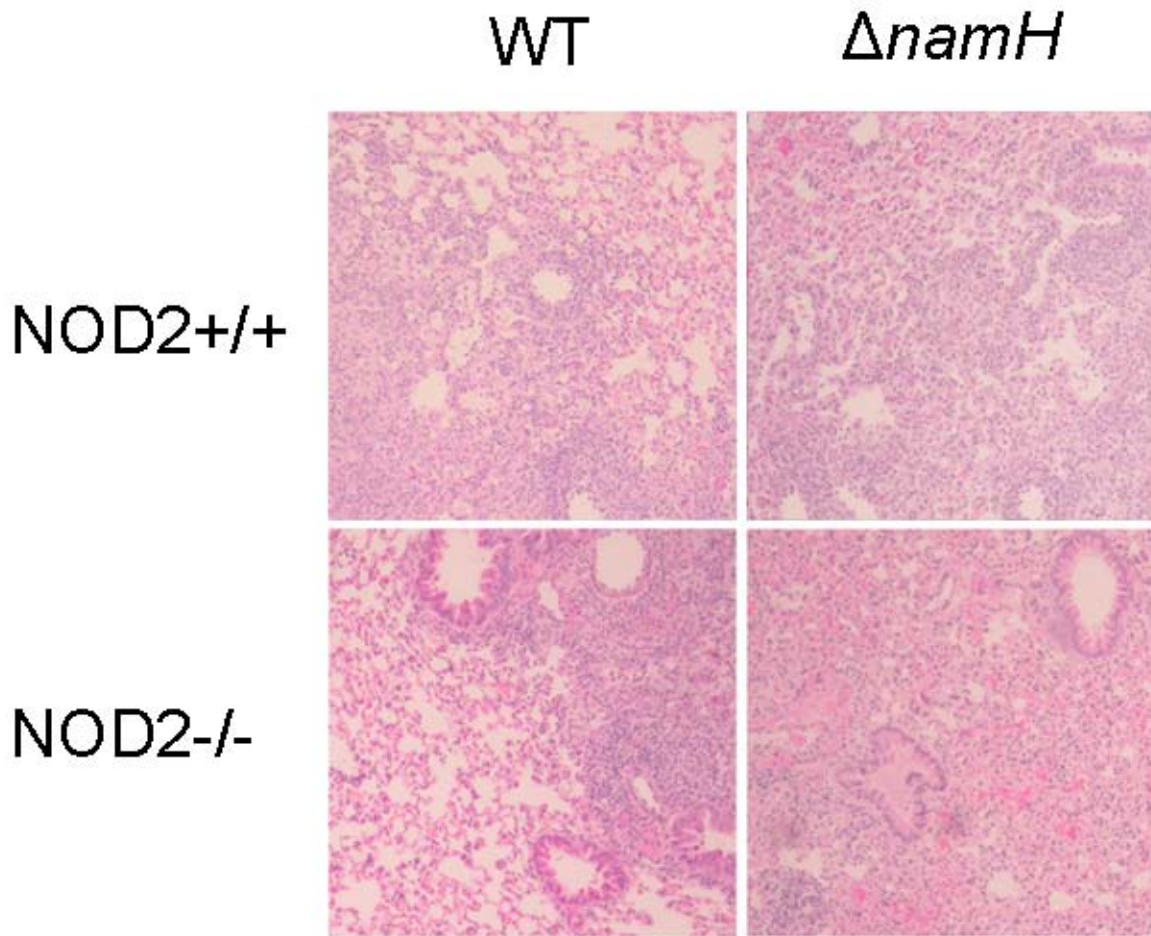


Figure 10. Histopathology of Nod2-deficient Mouse Lungs Infected with *Mtb*. Hematoxylin and eosin (H&E) stain of *Nod2*^{-/-} mouse lung sections and their *Nod2*^{+/+} littermates infected with *Mtb* wild-type H37Rv (WT) or the *namH* knockout ($\Delta namH$) at 3 weeks post-infection. Mice infected with WT strain show many well-defined granulomatous regions interspersed with healthy-looking lung tissue. Those mice infected with the *namH* knockout strain showed a much less organized lymphocytic infiltration phenotype and a diffuse neutrophilic pneumonitis. The *Nod2*^{-/-} mice infected with the *namH* knockout strain showed significantly less lymphocytic infiltration and very little healthy lung regions. Magnification is 100X.

growth within the lungs or spleen at either of the time points examined. Upon histopathological analysis, we observed a very surprising and interesting phenotype. *Nod2*^{-/-} mice infected with H37Rv wild-type at 3 weeks post-infection had as many well-defined lymphocytic infiltrations as in the *Nod2*^{+/+} mice, and had large interspersed regions of healthy lung (**Fig. 10**). Those *Nod2*^{-/-} mice infected with the *namH* knockout strain, however, had extremely low lymphocytic infiltration and strongly diffuse eosinophilic staining regions. The lungs of the *Nod2*^{-/-} and *Nod2*^{+/+} mice infected with the *namH* knockout were markedly different in that the latter had extensive lymphocytic infiltration, albeit diffusely organized. This observation that *Nod2*-deficient mice can respond strongly immunologically against H37Rv wild-type, but not against the *namH* knockout strain, implies the existence of an as-of-yet unidentified receptor for N-glycolyl MDP that certainly merits further investigation.

3.8: Rag knock-out mice study

To test the effect of *namH* disruption on innate immune responses, we infected *Rag1*^{-/-} mice (lacking the VDJ recombination capacity that permits an adaptive immune response [120]) with the aforementioned three strains of *Mtb* (**Fig. 11**). We observed that mice infected with H37Rv had a progressive infection that required compassionate sacrifice at a median time of 36 days post-infection, which was significantly different ($p < 0.0004$) from mice infected with the *namH* knockout strain which had a median survival time of 51 days. Furthermore, mice infected with the complement strain lived significantly longer ($p < 0.0025$) than those infected with the *namH* knockout strain (median of 45 days). Overall the $\Delta namH$ strain was reduced in virulence.

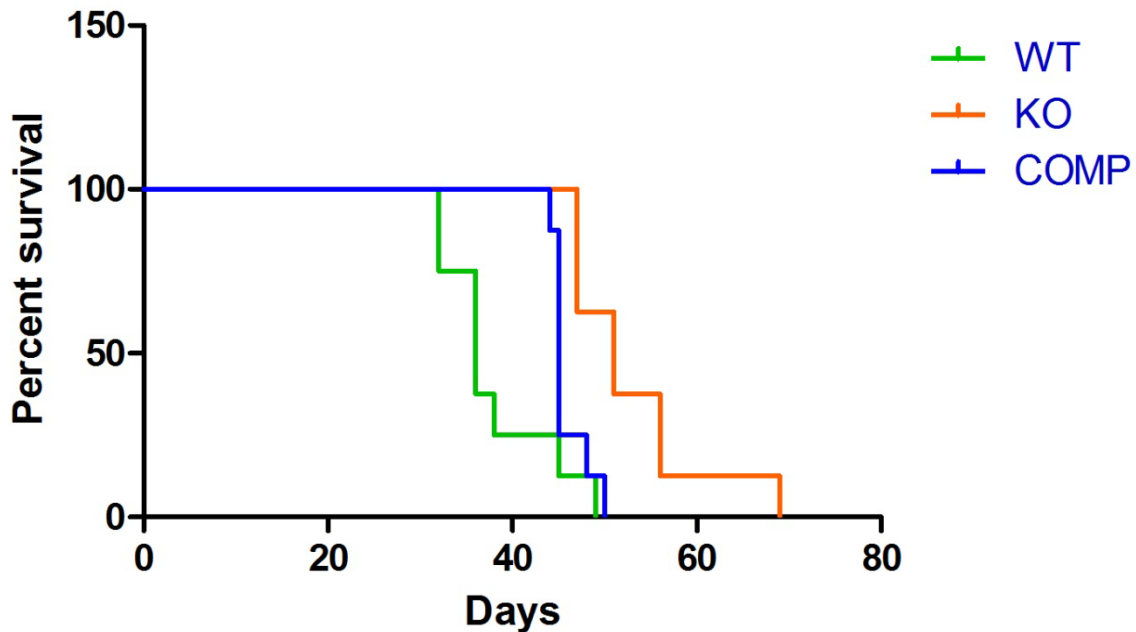


Figure 11. Survival Study of Mice Infected with *Mtb*. Rag1^{-/-} mice, which lack an intact adaptive immune response, were aerosol infected as previously described with three strains of *Mtb*: wild-type H37Rv (WT), the *namH* knockout (KO), and the complement under the native promoter (Comp). Approximately 34 CFU were implanted into the lungs of the mice infected with WT strain, 51 CFU for the KO strain and 97 CFU for the complement strain. Median survival times were as follows: WT (36 days), KO (51 days) and Comp (45 days). There were significant differences ($P < 0.005$) between both WT and KO comparisons and Comp and KO comparisons. Eight mice were used per group. Significance values were obtained using the log-rank test.

Part 4: Discussion

4.1 The Role of MDP in Immunity

The *N*-glycolyl modification of MDP seems to be a unique evolution in the cell wall of mycobacteria in that its function seems to be to promote inflammation and alert the host of its presence. Since all strains isolated to date maintain an intact *namH* locus [108], and given that disruption of *namH* seems to have no obvious detrimental effects on viability (our study), this argues that the main purpose of this modification is to elicit an immune response in the host. This conclusion, as paradoxical as it may seem, immediately demands an explanation. In contrast to most pathogens, it has been observed that T cell epitopes in non-essential proteins of *Mtb* have had an extremely high tendency to be conserved throughout *Mtb*-human co-evolution [121]. Comas et al 2010 argued that the conservation of epitopes is explained because certain T cell responses may be detrimental to the host and increases the likelihood of transmission, which outweighs any risk posed to *Mtb* by maintaining strong immunogenicity [121]. There is evidence that in HIV for example, there may have been an evolution in a similar way to promote its transmission rather than *in vivo* replication [122]. Furthermore, it seems that *Mtb* is not the only pathogen to adapt such a distinct immune subversion strategy: *Salmonella typhi* [123] and *Chlamydia trachomatis* [124] also demonstrate a lack of antigenic variability, perhaps reflecting a mechanism of survival and/or transmission similar to *Mtb*.

4.2 Inflammatory Response

Our studies have clearly demonstrated that the disruption of the *namH* gene in *Mtb* not only eliminates entirely the presence of *N*-glycolated muropeptides in the PGN but also that the bacteria are otherwise unaltered and viable, providing us with a tool to study exclusively the immunological properties of the *N*-glycolyl modification in virulent mycobacterial infection. It is convenient that we have not observed any differences in bacterial burden in mice lungs up until 12 weeks post-infection, which may mean that the main quality we are studying is the immunogenicity of PGN rather than bacterial viability. As was observed in the early time points, there is a phenotype of diffuse neutrophilic pneumonitis induced by the *namH* knockout strain in the lungs of infected mice, a finding that certainly requires confirmation by immunohistochemistry or FACS analysis. If it is reproducible, we must aim to identify the cause of such a difference in the *Mtb* lacking the immunogenic *N*-glycolyl MDP group. The role of INF- γ secreted by neutrophils has been shown to be a key factor in granuloma formation in non-mycobacterial infections, and it has also been demonstrated in non-mycobacterial infections that neutrophilic pneumonitis is MyD88 (and TLR2) dependent [125]. On the other hand, it has been demonstrated that mice entirely lacking neutrophils were no more susceptible to infection by any mycobacteria (including *Mtb*) compared to wild-type controls [126]. Furthermore, bacterial burden seems to be unaffected by the absence of neutrophils in *Mtb* infection [126]. Studies of inflammatory responses in the lungs of C57Bl/6 mice compared to A/J strain mice infected with virulent *Mtb* Erdman demonstrated a response similar to our study involving the *namH* knockout strain [127]. Remarkably, not only did the A/J mice succumb earlier to infection, but the lungs of the A/J mice were characterized by a diffuse interstitial pneumonitis composed of monocytes, lymphocytes and neutrophils in addition to diffuse bacteria; there were no clearly

defined granulomas observed [127]. In contrast, in the C57Bl/6 mice there was a delayed but persistent granuloma formation containing most of the bacteria, but only mild interstitial inflammation. This diffuse interstitial inflammation is precisely what we observed at two weeks in the *namH* knockout strain, as well as the defined granulomas interspersed by clear airways in the mice infected with wild-type and complement strains.

It is interesting to attempt to predict the future outcome of infections with the *namH*-deficient strain, as after a short time the diffuse inflammation in the A/J mice resolved and was replaced by focal granulomas [127]. By the same token, if we continue along this line of reasoning, we should predict that mice infected with the *namH* knockout strain in our DBA2-C57BL/6 mice engaged in the survival study should succumb earlier to their infection. Throughout the infections of the A/J and C57BL/6 mice, the inflammatory cytokines such as TNF- α , INF- γ , IL-6 and IL-1 β were much lower in the A/J mice, except for the initial period of infection where cytokine levels were substantially higher [127]. Also consistent with our findings was the observation that *Mtb* replicated equally well in both A/J and C57Bl/6 mice [127]. The authors attributed the difference in A/J mice to elevated INF γ levels. It seems plausible that the reduced immunogenicity conferred upon the *namH*-deficient strain is leading to an A/J-like phenotype, while the overall effect on survival is still unknown. Perhaps *N*-glycolyl muramic acid has a role in *Mtb* infection that elicits an immune response from the host, leading to granuloma formation to contain bacteria, which ultimately seems to be beneficial to both organisms as a symbiotic relationship. Although the A/J mouse model of *Mtb* infection is clearly different from the *namH*-deficient model of infection, there may be lessons we can take from the former to help better understand the latter, and perhaps *vice versa*, since the resulting pathological phenotype seems similar thus far. As a priority we must therefore not only identify

and quantitatively measure the cells in the lungs of mice infected with *namH*-deficient *Mtb* but also quantify the cytokines, especially INF- γ , at early and late time points.

4.3: PAMPs and PRRs

In an attempt to put our findings into context of general bacterial PAMP interactions with PRRs, it can be useful to look at other examples of their genetic disruption. It is interesting to examine how the disruption of a PRR in the host or the corresponding PAMP in the pathogen may have completely opposing effects. In order to conduct a precise analogous comparison with disruption of the *N*-glycolyl muramic acid PAMP we should look for another *Mtb* PAMP that has as close a function as possible: one that has a main and perhaps exclusive function of stimulating an immune response. One PAMP that we may consider is the 19-kDa lipoprotein (also called LpqH) that is identified by TLR2 and is a potent immunostimulator [128]. Deletion of 19-kDa lipoprotein from *Mtb* resulted in mildly reduced bacterial burden in mice at early (2 weeks) and later time (8 weeks) points [129]. A 19-kDa lipoprotein knockout strain also induced less IL12-p40 and IL-1 β from monocyte-derived macrophages [128] and has been shown to induce an NF- κ B response in a TLR2-dependent fashion [130]. Unfortunately the 19-kDa lipoprotein does more than stimulate an immune response in the host, as it has also been demonstrated to reduce MHC-II expression and antigen processing. On the other hand, perhaps this latter effect is common to most PAMPs, as it has also been observed that LPS or CpG DNA can induce a strong inflammatory response while inhibiting MHC-II expression [131]. Perhaps this reflects an evolved mechanism to counteract host PRR development. Therefore it may also be interesting to investigate if *N*-glycolyl muramic acid inhibits antigen processing in the host as

well. It may be that *Mtb* invades host macrophages and induces inflammatory cytokines in order to recruit potential vessels of infection (more macrophages), yet by inhibiting MHC-II maturation it does not permit the macrophage to identify to CD4⁺ cells which macrophages are infected. Conversely, in TLR2-knockout mice infected with wild-type *Mtb*, at 12 weeks post-infection their lungs showed larger granulomas and more neutrophilic infiltration, and there was lower NF-κB mediated cytokine responses [132]. Other studies showed TLR2-knockout mice succumbed slightly sooner than WT mice upon *Mtb* infection [133,134]. Therefore the disruption of the PAMP was associated with a disadvantage in *Mtb* while the disruption of the PRR was associated with a disadvantage for the host, perhaps indicating some evolved system of symbiosis where it is mutually beneficial to have PAMP-PRR recognition.

As another example of a mycobacterial PAMP that induces inflammation is Cord factor (TDM) that has been shown to interact with the macrophage-inducible c-type lectin (Mincle) [25]. TDM was shown to induce strong inflammatory responses in macrophages and in mice, an effect which was abolished in the absence of the Mincle receptor [25]. Unfortunately, *in vivo* data are lacking, but future experiments will surely provide insight into the function of the highly immunogenic molecules such as TDM contained within the *Mtb* cell wall. There also exist soluble immunostimulators such as the soluble tuberculosis factor (STF) that has been shown to activate cells in a TLR-2 dependent fashion [135]. In contrast, some PAMPs such as ManLAM, which binds DC-SIGN or Mannose receptors [35,36], may be modified in mycobacteria to reduce immunogenicity and increase toxicity to the cell [27]. Given the current lag of research on the role of immunostimulatory PAMPs in the pathogenesis of *Mtb* infection, it is clear that in order to gain a better understanding of host-pathogen interactions we must not only identify these

PAMP/PRR pairs, but systematically test their disruption singly or in conjunction in the *in vivo* environment.

4.4: An Unidentified Receptor of *N*-glycolyl Muramic Acid

Of all the findings so far, perhaps the most intriguing is the possibility of another, unidentified receptor that is specific for *N*-glycolyl MDP. This hypothesis was derived from observations that there is an apparent *namH*-dependent inflammatory response in a *Nod2*^{-/-} context. Given that there are already two receptors identified for the native muramic acid molecule, Nod1 which detects the proximal 3 amino acids and Nod2 which detects the muramic acid and proximal 2 peptides [136], it seems reasonable there could be a third as-of-yet unidentified receptor to this potent immunostimulatory molecule. In addition, perhaps the study of different cell types such a dendritic cells may reveal this unidentified receptor, in much the same way as the mannosylated LAM (ManLAM) PAMP has been identified to be detected by mannose receptors on macrophages [35] or DC-SIGN receptors on dendritic cells [36].

4.5: The Complement Strain

An important caveat in interpreting the data from the *namH* knockout strain is hinted at by the observation that the complement strain did not always complement fully, or sometimes not at all. Given that we observed a full return of *N*-glycolated muramic acid in the complement strains as measured by HPLC, there are at least three possible explanations for the failed

complementation in murine bacterial burden experiments: 1) *namH* expression is regulated *in vivo* during different stages of infection, and our non-specific integration vector removed *namH* from this regulation operon, 2) the CFUs calculated were artificially low due to technical and biological variability, or 3) the significantly higher CFU in mice infected with the wild-type strain was artificially high due to technical and biological variability. In order to test for the first possibility, we are currently conducting ongoing experiments examining *namH* mRNA levels in *M. bovis* BCG during different growth phases *in vitro*. Furthermore, we aim to test *namH* expression under a tet-inducible promoter in the *namH* knockout *Mtb* strain at both early and late points of infection in order to better understand the role of *N*-glycolyl MDP under these conditions. It is already known that *namH* expression is variable, for example in *Rhodococcus rhodochrous*, *namH* activity seems to be dependent on growth conditions, and when glycerol is added to the cultures *N*-glycolation of muramic acid was suppressed until the later stages of growth [104]. It seems the second possibility is a more likely explanation for partially-failed complementation given the HPLC results confirmed *N*-glycolyl muropeptides, as well as histopathology and studies in *Rag1*^{-/-} mice confirmed complementation.

It may also be possible that we inadvertently disrupted a flanking gene of *namH* in addition to the desired knockout, and thus complementation of Rv3818 would be insufficient to restore full genetic integrity. In light of this possibility, it should be noted that the genes that flank *namH* (3817 upstream, and 3819 downstream) are both predicted to be non-essential for growth *in vivo* when studied for up to 8 weeks [129]. As we observed significantly decreased splenic bacterial burden in the knockout and complement strains at 6 weeks post-infection, it seems unlikely that impaired expression of either of these genes is contributing to our observed phenotype. Importantly, the role of Rv3818 (*namH*) during *in vivo* survival was not able to be

conclusively resolved in this study. Furthermore, a mutation in Rv3817, which is hypothesized to be involved in cellular metabolism [110], does not seem to provide a satisfactory explanation for the histopathological phenotypes we have observed. On the other hand, the function of Rv3819 is still unknown in *Mtb* as well as all of its known orthologs, and the possibility that it comprises an operon with Rv3818 is still unresolved. Nonetheless, if lack of complementation persists with more stringent experimental conditions, the genomic DNA of the surrounding genes in the *namH* knockout strain should be sequenced in order to discount the possibility of a mutation in their coding regions. Furthermore, a quantitative real-time PCR analysis of Rv3817-3819 should aid in identifying the existence of an operon.

4.6 Future Directions

There remain several questions to be addressed regarding the basic properties of the *namH* mutant strain as well as its immunogenic characteristics. Firstly, it should be conclusively demonstrated that an increased susceptibility to lysozyme cleavage is in no way attenuating our mutant strain. There is recent speculation [4] as well as weak evidence [101] that this is true, but the persistence of our *namH* strain *in vivo* for at least 6 weeks unhindered argues against any such susceptibility. On the other hand, perhaps a mild susceptibility early on could explain the observed increase in inflammation at 2 weeks as muramic acid residues are liberated from the cell wall. A second priority is to study the macrophage response to live *namH* knockout strain *Mtb*. It is known that virulent H37Rv *Mtb* are able to subvert the host immune response in macrophages to secrete less inflammatory cytokines than avirulent H37Ra or the attenuated *M. bovis* BCG [137]. If we observe that the *namH* knockout strain induces a higher cytokine

response in infected murine macrophages, this may partly contribute to the observed phenotype of increased inflammation in the lungs at 2 weeks post-infection. Incidentally, such an observation would also imply attenuation in the *namH* knockout strain. As previously mentioned, in order to quantify the difference in immune response between wild-type and *namH* knockout *Mtb*-infected lungs, we plan to perform a FACS analysis at early time-points of infection. In addition, we should do a whole-lipid extraction of the mycobacterial cell wall to test for any differences in mycolic acids, TDM, *etc.* that may be disrupted in the *namH* knockout strain, which would further rule-out any other confounding factors that could explain our observations.

For long-term studies of the effect of *namH* disruption we await results from C57Bl/6 mice infected for 12 and 18 weeks. Furthermore, in order to definitely define a role of *namH* in virulence we have infected DBA2-C57Bl6 hybrid mice, a strain that is slightly more susceptible to *Mtb* infection [118], in a survival study that is ongoing. Another experiment that could prove worthy is a four-part expression microarray study examining the “genetics-squared” approach to studying host-pathogen interactions involving *Nod2*^{+/+} or *Nod2*^{-/-} macrophages infected with either WT or *namH*-deficient *Mtb*. Such an experiment would not only provide us with an idea of cytokine changes that are *Nod2* or NamH dependent, but also may provide insight into what other receptors (if any) are capable of detecting *N*-glycolyl MDP. Certainly the results of each experiment will guide us in determining the appropriate experiments that should follow.

4.7 Conclusions

In conclusion we have shown that the disruption of *namH* in *Mtb* results in the complete elimination of *N*-glycolyl muramic acid incorporated into the PGN layer. Furthermore, we have demonstrated that the *namH* mutant is not only fully viable, but appears to have no alterations in morphology or growth kinetics. We have shown that it is possible to biochemically complement the *namH* knockout strain with a non-specific integrating vector, but also that an *hsp60*-driven *namH* complementation does not necessarily increase the ratio of *N*-glycolyl to *N*-acetyl muramic acid residues. Disruption of *namH* does not seem to have an effect on bacterial burden in the lungs of infected mice for at least 6 weeks post-infection, but it may be associated with a slight decrease in CFU at 12 weeks. Whether or not this trend continues will be the outcome of our ongoing infection scheduled to last 18 weeks. The *namH* knockout strain appears to induce a strongly diffuse neutrophilic pneumonitis as early as 2 weeks that seems to persist throughout the infection; it appears at 3 weeks that there are fewer granulomas in the *namH* knockout strain which is perhaps a consequence of the reduced immunogenicity in the PGN layer. Furthermore, our studies with *Nod2*-deficient mice hinted at the existence of an as-of-yet unidentified receptor for *N*-glycolyl muramic acid. Finally, we observed that infection of *Rag1*^{-/-} mice that lack an adaptive immune response succumbed to death at a later time when infected with the *namH*-deficient strain. Although these studies seem to have opened up more questions than they have answered, this is perhaps the true goal of any scientific investigation. We have examined the effect of eliminating Freund's complete adjuvant in the natural infection scenario, and we have observed an immunological phenotype. Upon further investigation, the results of the studies conducted herein will surely prove to be a stepping stone in understanding the way in which *M. tuberculosis* establishes persistent infections and causes disease.

References

1. Janeway CA, Jr.: **Approaching the asymptote? Evolution and revolution in immunology.** *Cold Spring Harb Symp Quant Biol* 1989, **54 Pt 1**:1-13.
2. Janeway CA, Jr.: **The immune system evolved to discriminate infectious nonself from noninfectious self.** *Immunol Today* 1992, **13**:11-16.
3. Medzhitov R, Janeway CA, Jr.: **Innate immunity: the virtues of a nonclonal system of recognition.** *Cell* 1997, **91**:295-298.
4. Netea MG, van der Meer JW: **Immunodeficiency and genetic defects of pattern-recognition receptors.** *N Engl J Med* 2011, **364**:60-70.
5. WHO: **World Health Organization (WHO) Report 2010: Global Tuberculosis Control.** 2010.
6. Azuma I, Yamamura Y, Fukushi K: **Fractionation of mycobacterial cell wall. Isolation of arabinose mycolate and arabinogalactan from cell wall fraction of Mycobacterium tuberculosis strain Aoyama B.** *J Bacteriol* 1968, **96**:1885-1887.
7. Lederer E: **The mycobacterial cell wall.** *Pure Appl Chem* 1971, **25**:135-165.
8. Adam A, Petit JF, Wietzerbin-Falszpan J, Sinay P, Thomas DW, Lederer E: **L'acide N-glycolylmuramique, Constituants Des Parois De Mycobacterium Smegmatis: Identification Par Spectrometrie De Masse.** *FEBS Lett* 1969, **4**:87-92.
9. Brennan PJ, Nikaido H: **The envelope of mycobacteria.** *Annu Rev Biochem* 1995, **64**:29-63.
10. Ghuysen JM: **Use of bacteriolytic enzymes in determination of wall structure and their role in cell metabolism.** *Bacteriol Rev* 1968, **32**:425-464.
11. Schleifer KH, Kandler O: **Peptidoglycan types of bacterial cell walls and their taxonomic implications.** *Bacteriol Rev* 1972, **36**:407-477.
12. Hett EC, Rubin EJ: **Bacterial growth and cell division: a mycobacterial perspective.** *Microbiol Mol Biol Rev* 2008, **72**:126-156, table of contents.
13. Wietzerbin J, Das BC, Petit JF, Lederer E, Leyh-Bouille M, Ghuysen JM: **Occurrence of D-alanyl-(D)-meso-diaminopimelic acid and meso-diaminopimelyl-meso-diaminopimelic acid interpeptide linkages in the peptidoglycan of Mycobacteria.** *Biochemistry* 1974, **13**:3471-3476.
14. Azuma I, Thomas DW, Adam A, Ghuysen JM, Bonaly R, Petit JF, Lederer E: **Occurrence of N-glycolylmuramic acid in bacterial cell walls. A preliminary survey.** *Biochim Biophys Acta* 1970, **208**:444-451.
15. Petit JF, Adam A, Wietzerbin-Falszpan J, Lederer E, Ghuysen JM: **Chemical structure of the cell wall of Mycobacterium smegmatis. I. Isolation and partial characterization of the peptidoglycan.** *Biochem Biophys Res Commun* 1969, **35**:478-485.

16. Lederer E, Adam A, Ciorbaru R, Petit JF, Wietzerbin J: **Cell walls of Mycobacteria and related organisms; chemistry and immunostimulant properties.** *Mol Cell Biochem* 1975, **7**:87-104.
17. Mahapatra S, Crick DC, McNeil MR, Brennan PJ: **Unique structural features of the peptidoglycan of Mycobacterium leprae.** *J Bacteriol* 2008, **190**:655-661.
18. McNeil M, Daffe M, Brennan PJ: **Evidence for the nature of the link between the arabinogalactan and peptidoglycan of mycobacterial cell walls.** *J Biol Chem* 1990, **265**:18200-18206.
19. Daffe M, Brennan PJ, McNeil M: **Predominant structural features of the cell wall arabinogalactan of Mycobacterium tuberculosis as revealed through characterization of oligoglycosyl alditol fragments by gas chromatography/mass spectrometry and by ¹H and ¹³C NMR analyses.** *J Biol Chem* 1990, **265**:6734-6743.
20. Misaki A, Seto N, Azuma I: **Structure and immunological properties of D-arabino-D-galactans isolated from cell walls of Mycobacterium species.** *J Biochem* 1974, **76**:15-27.
21. Azuma I, Yamamura Y, Misaki A: **Isolation and characterization of arabinose mycolate from firmly bound lipids of mycobacteria.** *J Bacteriol* 1969, **98**:331-333.
22. Brennan PJ: **Structure, function, and biogenesis of the cell wall of Mycobacterium tuberculosis.** *Tuberculosis (Edinb)* 2003, **83**:91-97.
23. Spargo BJ, Crowe LM, Ionedo T, Beaman BL, Crowe JH: **Cord factor (alpha,alpha-trehalose 6,6'-dimycolate) inhibits fusion between phospholipid vesicles.** *Proc Natl Acad Sci U S A* 1991, **88**:737-740.
24. Schoenen H, Bodendorfer B, Hitchens K, Manzanero S, Werninghaus K, Nimmerjahn F, Agger EM, Stenger S, Andersen P, Ruland J, et al.: **Cutting edge: Mincle is essential for recognition and adjuvanticity of the mycobacterial cord factor and its synthetic analog trehalose-dibehenate.** *J Immunol* 2010, **184**:2756-2760.
25. Ishikawa E, Ishikawa T, Morita YS, Toyonaga K, Yamada H, Takeuchi O, Kinoshita T, Akira S, Yoshikai Y, Yamasaki S: **Direct recognition of the mycobacterial glycolipid, trehalose dimycolate, by C-type lectin Mincle.** *J Exp Med* 2009, **206**:2879-2888.
26. Chatterjee D, Khoo KH: **Mycobacterial lipoarabinomannan: an extraordinary lipoheteroglycan with profound physiological effects.** *Glycobiology* 1998, **8**:113-120.
27. Knutson KL, Hmama Z, Herrera-Velitz P, Rochford R, Reiner NE: **Lipoarabinomannan of Mycobacterium tuberculosis promotes protein tyrosine dephosphorylation and inhibition of mitogen-activated protein kinase in human mononuclear phagocytes. Role of the Src homology 2 containing tyrosine phosphatase 1.** *J Biol Chem* 1998, **273**:645-652.
28. Prinzi S, Chatterjee D, Brennan PJ: **Structure and antigenicity of lipoarabinomannan from Mycobacterium bovis BCG.** *J Gen Microbiol* 1993, **139**:2649-2658.
29. Ortalo-Magne A, Andersen AB, Daffe M: **The outermost capsular arabinomannans and other mannoconjugates of virulent and avirulent tubercle bacilli.** *Microbiology* 1996, **142** (Pt 4):927-935.

30. Chatterjee D, Lowell K, Rivoire B, McNeil MR, Brennan PJ: **Lipoarabinomannan of *Mycobacterium tuberculosis*. Capping with mannosyl residues in some strains.** *J Biol Chem* 1992, **267**:6234-6239.
31. Gilleron M, Himoudi N, Adam O, Constant P, Venisse A, Riviere M, Puzo G: ***Mycobacterium smegmatis* phosphoinositols-glyceroarabinomannans. Structure and localization of alkali-labile and alkali-stable phosphoinositides.** *J Biol Chem* 1997, **272**:117-124.
32. Chatterjee D, Roberts AD, Lowell K, Brennan PJ, Orme IM: **Structural basis of capacity of lipoarabinomannan to induce secretion of tumor necrosis factor.** *Infect Immun* 1992, **60**:1249-1253.
33. Roach TI, Barton CH, Chatterjee D, Liew FY, Blackwell JM: **Opposing effects of interferon-gamma on iNOS and interleukin-10 expression in lipopolysaccharide- and mycobacterial lipoarabinomannan-stimulated macrophages.** *Immunology* 1995, **85**:106-113.
34. Yoshida A, Koide Y: **Arabinofuranosyl-terminated and mannosylated lipoarabinomannans from *Mycobacterium tuberculosis* induce different levels of interleukin-12 expression in murine macrophages.** *Infect Immun* 1997, **65**:1953-1955.
35. Schlesinger LS: **Macrophage phagocytosis of virulent but not attenuated strains of *Mycobacterium tuberculosis* is mediated by mannose receptors in addition to complement receptors.** *J Immunol* 1993, **150**:2920-2930.
36. Tailleux L, Schwartz O, Herrmann JL, Pivert E, Jackson M, Amara A, Legres L, Dreher D, Nicod LP, Gluckman JC, et al.: **DC-SIGN is the major *Mycobacterium tuberculosis* receptor on human dendritic cells.** *J Exp Med* 2003, **197**:121-127.
37. Maeda N, Nigou J, Herrmann JL, Jackson M, Amara A, Lagrange PH, Puzo G, Gicquel B, Neyrolles O: **The cell surface receptor DC-SIGN discriminates between *Mycobacterium* species through selective recognition of the mannose caps on lipoarabinomannan.** *J Biol Chem* 2003, **278**:5513-5516.
38. van Kooyk Y, Appelmelk B, Geijtenbeek TB: **A fatal attraction: *Mycobacterium tuberculosis* and HIV-1 target DC-SIGN to escape immune surveillance.** *Trends Mol Med* 2003, **9**:153-159.
39. Cox JS, Chen B, McNeil M, Jacobs WR, Jr.: **Complex lipid determines tissue-specific replication of *Mycobacterium tuberculosis* in mice.** *Nature* 1999, **402**:79-83.
40. Camacho LR, Ensergueix D, Perez E, Gicquel B, Guilhot C: **Identification of a virulence gene cluster of *Mycobacterium tuberculosis* by signature-tagged transposon mutagenesis.** *Mol Microbiol* 1999, **34**:257-267.
41. Astarie-Dequeker C, Le Guyader L, Malaga W, Seaphanh FK, Chalut C, Lopez A, Guilhot C: **Phthiocerol dimycocerosates of *M. tuberculosis* participate in macrophage invasion by inducing changes in the organization of plasma membrane lipids.** *PLoS Pathog* 2009, **5**:e1000289.
42. Gatfield J, Pieters J: **Essential role for cholesterol in entry of mycobacteria into macrophages.** *Science* 2000, **288**:1647-1650.

43. Maldonado-Garcia G, Chico-Ortiz M, Lopez-Marin LM, Sanchez-Garcia FJ: **High-polarity Mycobacterium avium-derived lipids interact with murine macrophage lipid rafts.** *Scand J Immunol* 2004, **60**:463-470.
44. Rousseau C, Winter N, Pivert E, Bordat Y, Neyrolles O, Ave P, Huerre M, Gicquel B, Jackson M: **Production of phthiocerol dimycocerosates protects Mycobacterium tuberculosis from the cidal activity of reactive nitrogen intermediates produced by macrophages and modulates the early immune response to infection.** *Cell Microbiol* 2004, **6**:277-287.
45. Domenech P, Reed MB: **Rapid and spontaneous loss of phthiocerol dimycocerosate (PDIM) from Mycobacterium tuberculosis grown in vitro: implications for virulence studies.** *Microbiology* 2009, **155**:3532-3543.
46. Girardin SE, Boneca IG, Carneiro LA, Antignac A, Jehanno M, Viala J, Tedin K, Taha MK, Labigne A, Zahringer U, et al.: **Nod1 detects a unique muropeptide from gram-negative bacterial peptidoglycan.** *Science* 2003, **300**:1584-1587.
47. Chamaillard M, Hashimoto M, Horie Y, Masumoto J, Qiu S, Saab L, Ogura Y, Kawasaki A, Fukase K, Kusumoto S, et al.: **An essential role for NOD1 in host recognition of bacterial peptidoglycan containing diaminopimelic acid.** *Nat Immunol* 2003, **4**:702-707.
48. Inohara N, Ogura Y, Chen FF, Muto A, Nunez G: **Human Nod1 confers responsiveness to bacterial lipopolysaccharides.** *J Biol Chem* 2001, **276**:2551-2554.
49. Girardin SE, Boneca IG, Viala J, Chamaillard M, Labigne A, Thomas G, Philpott DJ, Sansonetti PJ: **Nod2 is a general sensor of peptidoglycan through muramyl dipeptide (MDP) detection.** *J Biol Chem* 2003, **278**:8869-8872.
50. Inohara N, Koseki T, del Peso L, Hu Y, Yee C, Chen S, Carrio R, Merino J, Liu D, Ni J, et al.: **Nod1, an Apaf-1-like activator of caspase-9 and nuclear factor-kappaB.** *J Biol Chem* 1999, **274**:14560-14567.
51. Bertin J, Nir WJ, Fischer CM, Tayber OV, Errada PR, Grant JR, Keilty JJ, Gosselin ML, Robison KE, Wong GH, et al.: **Human CARD4 protein is a novel CED-4/Apaf-1 cell death family member that activates NF-kappaB.** *J Biol Chem* 1999, **274**:12955-12958.
52. Franchi L, Warner N, Viani K, Nunez G: **Function of Nod-like receptors in microbial recognition and host defense.** *Immunol Rev* 2009, **227**:106-128.
53. Ogura Y, Inohara N, Benito A, Chen FF, Yamaoka S, Nunez G: **Nod2, a Nod1/Apaf-1 family member that is restricted to monocytes and activates NF-kappaB.** *J Biol Chem* 2001, **276**:4812-4818.
54. Tanabe T, Chamaillard M, Ogura Y, Zhu L, Qiu S, Masumoto J, Ghosh P, Moran A, Predergast MM, Tromp G, et al.: **Regulatory regions and critical residues of NOD2 involved in muramyl dipeptide recognition.** *EMBO J* 2004, **23**:1587-1597.
55. Inohara N, Koseki T, Lin J, del Peso L, Lucas PC, Chen FF, Ogura Y, Nunez G: **An induced proximity model for NF-kappa B activation in the Nod1/RICK and RIP signaling pathways.** *J Biol Chem* 2000, **275**:27823-27831.

56. Kobayashi K, Inohara N, Hernandez LD, Galan JE, Nunez G, Janeway CA, Medzhitov R, Flavell RA: **RICK/Rip2/CARDIAK mediates signalling for receptors of the innate and adaptive immune systems.** *Nature* 2002, **416**:194-199.
57. Abbott DW, Wilkins A, Asara JM, Cantley LC: **The Crohn's disease protein, NOD2, requires RIP2 in order to induce ubiquitinylation of a novel site on NEMO.** *Curr Biol* 2004, **14**:2217-2227.
58. Thome M, Hofmann K, Burns K, Martinon F, Bodmer JL, Mattmann C, Tschopp J: **Identification of CARDIAK, a RIP-like kinase that associates with caspase-1.** *Curr Biol* 1998, **8**:885-888.
59. Hayden MS, Ghosh S: **Signaling to NF-kappaB.** *Genes Dev* 2004, **18**:2195-2224.
60. Kobe B, Deisenhofer J: **Proteins with leucine-rich repeats.** *Curr Opin Struct Biol* 1995, **5**:409-416.
61. Ogura Y, Bonen DK, Inohara N, Nicolae DL, Chen FF, Ramos R, Britton H, Moran T, Karaliuskas R, Duerr RH, et al.: **A frameshift mutation in NOD2 associated with susceptibility to Crohn's disease.** *Nature* 2001, **411**:603-606.
62. Bonen DK, Ogura Y, Nicolae DL, Inohara N, Saab L, Tanabe T, Chen FF, Foster SJ, Duerr RH, Brant SR, et al.: **Crohn's disease-associated NOD2 variants share a signaling defect in response to lipopolysaccharide and peptidoglycan.** *Gastroenterology* 2003, **124**:140-146.
63. Coulombe F, Divangahi M, Veyrier F, de Leseleuc L, Gleason JL, Yang Y, Kelliher MA, Pandey AK, Sasseti CM, Reed MB, et al.: **Increased NOD2-mediated recognition of N-glycolyl muramyl dipeptide.** *J Exp Med* 2009, **206**:1709-1716.
64. Divangahi M, Mostowy S, Coulombe F, Kozak R, Guillot L, Veyrier F, Kobayashi KS, Flavell RA, Gros P, Behr MA: **NOD2-deficient mice have impaired resistance to Mycobacterium tuberculosis infection through defective innate and adaptive immunity.** *J Immunol* 2008, **181**:7157-7165.
65. Gandotra S, Jang S, Murray PJ, Salgame P, Ehrt S: **Nucleotide-binding oligomerization domain protein 2-deficient mice control infection with Mycobacterium tuberculosis.** *Infect Immun* 2007, **75**:5127-5134.
66. Kramer M, Netea MG, de Jong DJ, Kullberg BJ, Adema GJ: **Impaired dendritic cell function in Crohn's disease patients with NOD2 3020insC mutation.** *J Leukoc Biol* 2006, **79**:860-866.
67. Kullberg BJ, Ferwerda G, de Jong DJ, Drenth JP, Joosten LA, Van der Meer JW, Netea MG: **Crohn's disease patients homozygous for the 3020insC NOD2 mutation have a defective NOD2/TLR4 cross-tolerance to intestinal stimuli.** *Immunology* 2008, **123**:600-605.
68. Ferwerda G, Girardin SE, Kullberg BJ, Le Bourhis L, de Jong DJ, Langenberg DM, van Crevel R, Adema GJ, Ottenhoff TH, Van der Meer JW, et al.: **NOD2 and toll-like receptors are nonredundant recognition systems of Mycobacterium tuberculosis.** *PLoS Pathog* 2005, **1**:279-285.

69. Inohara N, Ogura Y, Fontalba A, Gutierrez O, Pons F, Crespo J, Fukase K, Inamura S, Kusumoto S, Hashimoto M, et al.: **Host recognition of bacterial muramyl dipeptide mediated through NOD2. Implications for Crohn's disease.** *J Biol Chem* 2003, **278**:5509-5512.
70. Takahashi Y, Isuzugawa K, Murase Y, Imai M, Yamamoto S, Iizuka M, Akira S, Bahr GM, Momotani E, Hori M, et al.: **Up-regulation of NOD1 and NOD2 through TLR4 and TNF-alpha in LPS-treated murine macrophages.** *J Vet Med Sci* 2006, **68**:471-478.
71. Takada H, Yokoyama S, Yang S: **Enhancement of endotoxin activity by muramyl dipeptide.** *J Endotoxin Res* 2002, **8**:337-342.
72. Kufer TA, Sansonetti PJ: **Sensing of bacteria: NOD a lonely job.** *Curr Opin Microbiol* 2007, **10**:62-69.
73. Austin CM, Ma X, Graviss EA: **Common nonsynonymous polymorphisms in the NOD2 gene are associated with resistance or susceptibility to tuberculosis disease in African Americans.** *J Infect Dis* 2008, **197**:1713-1716.
74. Berrington WR, Macdonald M, Khadge S, Sapkota BR, Janer M, Hagge DA, Kaplan G, Hawn TR: **Common polymorphisms in the NOD2 gene region are associated with leprosy and its reactive states.** *J Infect Dis* 2010, **201**:1422-1435.
75. Miceli-Richard C, Lesage S, Rybojad M, Prieur AM, Manouvrier-Hanu S, Hafner R, Chamaillard M, Zouali H, Thomas G, Hugot JP: **CARD15 mutations in Blau syndrome.** *Nat Genet* 2001, **29**:19-20.
76. Hampe J, Cuthbert A, Croucher PJ, Mirza MM, Mascheretti S, Fisher S, Frenzel H, King K, Hasselmeier A, MacPherson AJ, et al.: **Association between insertion mutation in NOD2 gene and Crohn's disease in German and British populations.** *Lancet* 2001, **357**:1925-1928.
77. Hugot JP, Chamaillard M, Zouali H, Lesage S, Cezard JP, Belaiche J, Almer S, Tysk C, O'Morain CA, Gassull M, et al.: **Association of NOD2 leucine-rich repeat variants with susceptibility to Crohn's disease.** *Nature* 2001, **411**:599-603.
78. Behr MA, Divangahi M, Lalande JD: **What's in a name? The (mis)labelling of Crohn's as an autoimmune disease.** *Lancet* 2010, **376**:202-203.
79. Behr MA, Kapur V: **The evidence for Mycobacterium paratuberculosis in Crohn's disease.** *Curr Opin Gastroenterol* 2008, **24**:17-21.
80. Kobayashi KS, Chamaillard M, Ogura Y, Henegariu O, Inohara N, Nunez G, Flavell RA: **Nod2-dependent regulation of innate and adaptive immunity in the intestinal tract.** *Science* 2005, **307**:731-734.
81. Wehkamp J, Harder J, Weichenthal M, Schwab M, Schaffeler E, Schlee M, Herrlinger KR, Stallmach A, Noack F, Fritz P, et al.: **NOD2 (CARD15) mutations in Crohn's disease are associated with diminished mucosal alpha-defensin expression.** *Gut* 2004, **53**:1658-1664.

82. Petnicki-Ocwieja T, Hrncir T, Liu YJ, Biswas A, Hudcovic T, Tlaskalova-Hogenova H, Kobayashi KS: **Nod2 is required for the regulation of commensal microbiota in the intestine.** *Proc Natl Acad Sci U S A* 2009, **106**:15813-15818.
83. van Duist MM, Albrecht M, Podswiadek M, Giachino D, Lengauer T, Punzi L, De Marchi M: **A new CARD15 mutation in Blau syndrome.** *Eur J Hum Genet* 2005, **13**:742-747.
84. Chamainard M, Girardin SE, Viala J, Philpott DJ: **Nods, Nalps and Naip: intracellular regulators of bacterial-induced inflammation.** *Cell Microbiol* 2003, **5**:581-592.
85. Hisamatsu T, Suzuki M, Reinecker HC, Nadeau WJ, McCormick BA, Podolsky DK: **CARD15/NOD2 functions as an antibacterial factor in human intestinal epithelial cells.** *Gastroenterology* 2003, **124**:993-1000.
86. Opitz B, Puschel A, Schmeck B, Hocke AC, Rosseau S, Hammerschmidt S, Schumann RR, Suttorp N, Hippenstiel S: **Nucleotide-binding oligomerization domain proteins are innate immune receptors for internalized Streptococcus pneumoniae.** *J Biol Chem* 2004, **279**:36426-36432.
87. Kufer TA, Kremmer E, Banks DJ, Philpott DJ: **Role for erbin in bacterial activation of Nod2.** *Infect Immun* 2006, **74**:3115-3124.
88. Asano J, Tada H, Onai N, Sato T, Horie Y, Fujimoto Y, Fukase K, Suzuki A, Mak TW, Ohteki T: **Nucleotide oligomerization binding domain-like receptor signaling enhances dendritic cell-mediated cross-priming in vivo.** *J Immunol* 2010, **184**:736-745.
89. Shaw MH, Kamada N, Warner N, Kim YG, Nunez G: **The ever-expanding function of NOD2: autophagy, viral recognition, and T cell activation.** *Trends Immunol* 2011.
90. Mizushima N, Levine B, Cuervo AM, Klionsky DJ: **Autophagy fights disease through cellular self-digestion.** *Nature* 2008, **451**:1069-1075.
91. Deretic V: **Strange bedfellows expose ancient secrets of autophagy in immunity.** *Immunity* 2009, **30**:479-481.
92. Cooney R, Baker J, Brain O, Danis B, Pichulik T, Allan P, Ferguson DJ, Campbell BJ, Jewell D, Simmons A: **NOD2 stimulation induces autophagy in dendritic cells influencing bacterial handling and antigen presentation.** *Nat Med* 2010, **16**:90-97.
93. Travassos LH, Carneiro LA, Ramjeet M, Hussey S, Kim YG, Magalhaes JG, Yuan L, Soares F, Chea E, Le Bourhis L, et al.: **Nod1 and Nod2 direct autophagy by recruiting ATG16L1 to the plasma membrane at the site of bacterial entry.** *Nat Immunol* 2010, **11**:55-62.
94. Homer CR, Richmond AL, Rebert NA, Achkar JP, McDonald C: **ATG16L1 and NOD2 interact in an autophagy-dependent antibacterial pathway implicated in Crohn's disease pathogenesis.** *Gastroenterology* 2010, **139**:1630-1641, 1641 e1631-1632.
95. Hampe J, Franke A, Rosenstiel P, Till A, Teuber M, Huse K, Albrecht M, Mayr G, De La Vega FM, Briggs J, et al.: **A genome-wide association scan of nonsynonymous SNPs identifies a susceptibility variant for Crohn disease in ATG16L1.** *Nat Genet* 2007, **39**:207-211.

96. Parkes M, Barrett JC, Prescott NJ, Tremelling M, Anderson CA, Fisher SA, Roberts RG, Nimmo ER, Cummings FR, Soars D, et al.: **Sequence variants in the autophagy gene IRGM and multiple other replicating loci contribute to Crohn's disease susceptibility.** *Nat Genet* 2007, **39**:830-832.
97. Gateau O, Bordet C, Michel G: **[Study of the formation of N-glycolylmuramic acid from Nocardia asteroides (author's transl)].** *Biochim Biophys Acta* 1976, **421**:395-405.
98. Essers L, Schoop HJ: **Evidence for the incorporation of molecular oxygen, a pathway in biosynthesis of N-glycolylmuramic acid in Mycobacterium phlei.** *Biochim Biophys Acta* 1978, **544**:180-184.
99. Vollmer W: **Structural variation in the glycan strands of bacterial peptidoglycan.** *FEMS Microbiol Rev* 2008, **32**:287-306.
100. Mahapatra S, Scherman H, Brennan PJ, Crick DC: **N Glycolylation of the nucleotide precursors of peptidoglycan biosynthesis of Mycobacterium spp. is altered by drug treatment.** *J Bacteriol* 2005, **187**:2341-2347.
101. Raymond JB, Mahapatra S, Crick DC, Pavelka MS, Jr.: **Identification of the namH gene, encoding the hydroxylase responsible for the N-glycolylation of the mycobacterial peptidoglycan.** *J Biol Chem* 2005, **280**:326-333.
102. Angata T, Varki A: **Chemical diversity in the sialic acids and related alpha-keto acids: an evolutionary perspective.** *Chem Rev* 2002, **102**:439-469.
103. Holt J. G. K, N. R., Sneath, P. H. A., Staley, J. T., and Williams, S. T.: *Bergey's Manual of Determinative Bacteriology* edn 9th. Baltimore: Williams & Wilkins; 1994.
104. Sutcliffe IC: **Cell envelope composition and organisation in the genus Rhodococcus.** *Antonie Van Leeuwenhoek* 1998, **74**:49-58.
105. Uchida KaA, K.: **Taxonomic significance of cell-wall acyl type in Corynebacterium-Mycobacterium-Nocardia group by a glycolate test.** *J. Gen. Appl. Microbiol.* 1979, **25**:169-183.
106. Uchida K, Kudo T, Suzuki KI, Nakase T: **A new rapid method of glycolate test by diethyl ether extraction, which is applicable to a small amount of bacterial cells of less than one milligram.** *J Gen Appl Microbiol* 1999, **45**:49-56.
107. Cole ST, Eiglmeier K, Parkhill J, James KD, Thomson NR, Wheeler PR, Honore N, Garnier T, Churcher C, Harris D, et al.: **Massive gene decay in the leprosy bacillus.** *Nature* 2001, **409**:1007-1011.
108. Tsolaki AG, Hirsh AE, DeRiemer K, Enciso JA, Wong MZ, Hannan M, Goguet de la Salmoniere YO, Aman K, Kato-Maeda M, Small PM: **Functional and evolutionary genomics of Mycobacterium tuberculosis: insights from genomic deletions in 100 strains.** *Proc Natl Acad Sci U S A* 2004, **101**:4865-4870.

109. Sasseti CM, Boyd DH, Rubin EJ: **Comprehensive identification of conditionally essential genes in mycobacteria.** *Proc Natl Acad Sci U S A* 2001, **98**:12712-12717.
110. Sasseti CM, Boyd DH, Rubin EJ: **Genes required for mycobacterial growth defined by high density mutagenesis.** *Mol Microbiol* 2003, **48**:77-84.
111. Rengarajan J, Bloom BR, Rubin EJ: **Genome-wide requirements for Mycobacterium tuberculosis adaptation and survival in macrophages.** *Proc Natl Acad Sci U S A* 2005, **102**:8327-8332.
112. Ellouz F, Adam A, Ciorbaru R, Lederer E: **Minimal structural requirements for adjuvant activity of bacterial peptidoglycan derivatives.** *Biochem Biophys Res Commun* 1974, **59**:1317-1325.
113. Kotani S, Watanabe Y, Kinoshita F, Shimono T, Morisaki I: **Immunoadjuvant activities of synthetic N-acetyl-muramyl-peptides or -amino acids.** *Biken J* 1975, **18**:105-111.
114. Snapper SB, Melton RE, Mustafa S, Kieser T, Jacobs WR, Jr.: **Isolation and characterization of efficient plasmid transformation mutants of Mycobacterium smegmatis.** *Mol Microbiol* 1990, **4**:1911-1919.
115. Pelicic V, Jackson M, Reyrat JM, Jacobs WR, Jr., Gicquel B, Guilhot C: **Efficient allelic exchange and transposon mutagenesis in Mycobacterium tuberculosis.** *Proc Natl Acad Sci U S A* 1997, **94**:10955-10960.
116. van Soolingen D, Hermans PW, de Haas PE, Soll DR, van Embden JD: **Occurrence and stability of insertion sequences in Mycobacterium tuberculosis complex strains: evaluation of an insertion sequence-dependent DNA polymorphism as a tool in the epidemiology of tuberculosis.** *J Clin Microbiol* 1991, **29**:2578-2586.
117. Slayden RAB, C. E. : **Analysis of the Lipids of Mycobacterium tuberculosis.** *METHODS IN MOLECULAR MEDICINE* 2001, **54**:229-246.
118. Medina E, North RJ: **Resistance ranking of some common inbred mouse strains to Mycobacterium tuberculosis and relationship to major histocompatibility complex haplotype and Nramp1 genotype.** *Immunology* 1998, **93**:270-274.
119. Lewis KN, Liao R, Guinn KM, Hickey MJ, Smith S, Behr MA, Sherman DR: **Deletion of RD1 from Mycobacterium tuberculosis mimics bacille Calmette-Guerin attenuation.** *J Infect Dis* 2003, **187**:117-123.
120. Mombaerts P, Iacomini J, Johnson RS, Herrup K, Tonegawa S, Papaioannou VE: **RAG-1-deficient mice have no mature B and T lymphocytes.** *Cell* 1992, **68**:869-877.
121. Comas I, Chakravarti J, Small PM, Galagan J, Niemann S, Kremer K, Ernst JD, Gagneux S: **Human T cell epitopes of Mycobacterium tuberculosis are evolutionarily hyperconserved.** *Nat Genet* 2010, **42**:498-503.
122. Fraser C, Hollingsworth TD, Chapman R, de Wolf F, Hanage WP: **Variation in HIV-1 set-point viral load: epidemiological analysis and an evolutionary hypothesis.** *Proc Natl Acad Sci U S A* 2007, **104**:17441-17446.

123. Holt KE, Parkhill J, Mazzoni CJ, Roumagnac P, Weill FX, Goodhead I, Rance R, Baker S, Maskell DJ, Wain J, et al.: **High-throughput sequencing provides insights into genome variation and evolution in Salmonella Typhi.** *Nat Genet* 2008, **40**:987-993.
124. Nunes A, Nogueira PJ, Borrego MJ, Gomes JP: **Adaptive evolution of the Chlamydia trachomatis dominant antigen reveals distinct evolutionary scenarios for B- and T-cell epitopes: worldwide survey.** *PLoS One* 2010, **5**.
125. Nance SC, Yi AK, Re FC, Fitzpatrick EA: **MyD88 is necessary for neutrophil recruitment in hypersensitivity pneumonitis.** *J Leukoc Biol* 2008, **83**:1207-1217.
126. Seiler P, Aichele P, Raupach B, Odermatt B, Steinhoff U, Kaufmann SH: **Rapid neutrophil response controls fast-replicating intracellular bacteria but not slow-replicating Mycobacterium tuberculosis.** *J Infect Dis* 2000, **181**:671-680.
127. Actor JK, Olsen M, Jagannath C, Hunter RL: **Relationship of survival, organism containment, and granuloma formation in acute murine tuberculosis.** *J Interferon Cytokine Res* 1999, **19**:1183-1193.
128. Stewart GR, Wilkinson KA, Newton SM, Sullivan SM, Neyrolles O, Wain JR, Patel J, Pool KL, Young DB, Wilkinson RJ: **Effect of deletion or overexpression of the 19-kilodalton lipoprotein Rv3763 on the innate response to Mycobacterium tuberculosis.** *Infect Immun* 2005, **73**:6831-6837.
129. Sasseti CM, Rubin EJ: **Genetic requirements for mycobacterial survival during infection.** *Proc Natl Acad Sci U S A* 2003, **100**:12989-12994.
130. Noss EH, Pai RK, Sellati TJ, Radolf JD, Belisle J, Golenbock DT, Boom WH, Harding CV: **Toll-like receptor 2-dependent inhibition of macrophage class II MHC expression and antigen processing by 19-kDa lipoprotein of Mycobacterium tuberculosis.** *J Immunol* 2001, **167**:910-918.
131. Chu RS, Askew D, Noss EH, Tobian A, Krieg AM, Harding CV: **CpG oligodeoxynucleotides down-regulate macrophage class II MHC antigen processing.** *J Immunol* 1999, **163**:1188-1194.
132. Sugawara I, Yamada H, Li C, Mizuno S, Takeuchi O, Akira S: **Mycobacterial infection in TLR2 and TLR6 knockout mice.** *Microbiol Immunol* 2003, **47**:327-336.
133. Tsolaki AG: **Innate immune recognition in tuberculosis infection.** *Adv Exp Med Biol* 2009, **653**:185-197.
134. Bafica A, Scanga CA, Feng CG, Leifer C, Cheever A, Sher A: **TLR9 regulates Th1 responses and cooperates with TLR2 in mediating optimal resistance to Mycobacterium tuberculosis.** *J Exp Med* 2005, **202**:1715-1724.
135. Means TK, Wang S, Lien E, Yoshimura A, Golenbock DT, Fenton MJ: **Human toll-like receptors mediate cellular activation by Mycobacterium tuberculosis.** *J Immunol* 1999, **163**:3920-3927.

136. Davis KM, Weiser JN: **Modifications to the peptidoglycan backbone help bacteria to establish infection.** *Infect Immun* 2011, **79**:562-570.
137. Falcone V, Bassey EB, Toniolo A, Conaldi PG, Collins FM: **Differential release of tumor necrosis factor-alpha from murine peritoneal macrophages stimulated with virulent and avirulent species of mycobacteria.** *FEMS Immunol Med Microbiol* 1994, **8**:225-232.

References for Figures

Figure 1. Schematic of the Mycobacterial Cell Wall. Jeffrey D Esko TLD, and Christian RH Raetz: *Essentials of Glycobiology* edn 2. **Figure 20.8.** Edited by Varki, Cummings, et al. The Consortium of Glycobiology Editors, La Jolla, California: Cold Spring Harbor Laboratory Press; 2009.

Figure 2A. NamH hydroxylation of MDP. Coulombe F, Divangahi M, Veyrier F, de Leseleuc L, Gleason JL, Yang Y, Kelliher MA, Pandey AK, Sasseti CM, Reed MB, et al.: **Increased NOD2-mediated recognition of N-glycolyl muramyl dipeptide.** *J Exp Med* 2009, **206**:1709-1716. Figure 1A.

APPENDIX I

Materials and Methods:

Peptidoglycan purification and solubilisation and HPLC Analysis

Samples were centrifuged at 39,000g for 30 min, and pellet was re-suspended in 20 ml of sterile H₂O. This process was repeated until no more SDS could be detected (see Hayashi et al. 1975). Samples were re-suspended in 10 ml of 0.5% KOH in methanol-diethyl ether (1/1) and stirred for 4 days at room temperature (RT) for hydrolyzing the mycolic acids (saponification). Samples were washed twice with methanol and re-suspended in 50mM Tris pH 7.0. Alpha-amylase (100µg/ml final concentration; Sigma) was added and incubated overnight (O/N) at 37°C. MgSO₄ (20mM final) and 20µl of DNase (1 mg.ml⁻¹) and 20µl of RNase (20 mg.ml⁻¹) was added and samples were incubated at 37°C for 2 hours. CaCl₂ (10mM final) and trypsin (100µg/ml final) were added to each sample. 8% SDS was added to each sample until a final concentration reached 1% (in a final volume of 1 ml) and was then boiled for 15 min. 20ml of sterile H₂O was added, and samples were centrifuged at 39,000g for 15 min. Pellet was re-suspended in 20ml sterile H₂O and centrifuged 39,000g for 15 min. Pellet was then re-suspended in 10ml LiCl₂ (8M) and incubated at 37°C for 15 min. 10ml of sterile H₂O was added and samples were centrifuged at 39,000g for 15 min. Pellet was dissolved in 10ml EDTA (100mM) and incubated at 37°C for 15 min. 10ml of sterile H₂O was added and samples were centrifuged at 39,000g for 15 min. Pellet was re-suspended in 20ml of sterile H₂O and centrifuged an additional 15 min at 39,000g. This step was done two times. Samples were then re-suspended in 10ml acetone and briefly sonicated in an ultrasonic bath, followed by centrifugation at 39,000g for 15 min. Samples were again washed by adding 20ml of sterile H₂O

and centrifuging at 39,000g for 15 min. 500µl of sterile H₂O was then added to the samples and lyophilized. Samples were then weighed (*H37Rv WT*: 14.8mg; *H37RvΔnamH*: 10.6mg; *H37RvΔnamH* complement: 12.4mg). In a polyallomer tube, 2ml of hydrofluoric acid (cooled to 4°C) was mixed with the samples and incubated with agitation for 4 days at 4°C. One millilitre of sample was then centrifuged at 45,000g for 30 min and supernatant discarded. The second millilitre was then added and centrifugation repeated. The sample pellet was then washed and centrifuged twice in 20ml of sterile H₂O, then twice in 50mM TrisHCL pH 7, then one more time in H₂O. Pellets were then resuspended in a small volume of H₂O and lyophilized. Samples were again weighed (*H37Rv WT*: 8.8mg; *H37RvΔnamH*: 5.5mg; *H37RvΔnamH* complement: 4.8mg) and H₂O was added in order to obtain a final concentration of 10mg PGN per ml. From this solution 200µg of each PGN sample were then treated with muramidase from *Streptomyces globisporus* (Sigma) as follows: 40µl PGN, 65µl H₂O, 15µl of 100 mM sodium phosphate buffer (pH 5.5), and 5µl muramidase enzyme. Mixture was incubated at 37°C for 16 hours with stirring. Equal volumes of 0.5M sodium-borate buffer (pH 9) and a pinch of sodium borohydride were added to a final concentration of 10mg/ml and incubated at RT to reduce sugar moieties. After 15 min, the reaction was stopped by addition of orthophosphoric acid (pH adjusted to pH 2, followed by centrifugation at 13000g for 1 min.

2.8: HPLC analysis of muropeptides

For HPLC fractionation, we used the Hypersil octyldecyl silane (C₁₈) column (4,6x250mm) connected to an Agilent 1100 HPLC system. Muropeptides were eluted with a methanol gradient of 0 to 15% (buffer A: 50mM NaH₂PO₄ pH=4.3 and buffer B 15% methanol, 75mM NaH₂PO₄) and the eluate monitored at 206nm. Some peaks were collected and de-salted with the

same system, but the muropeptides were eluted with an acetonitrile gradient of 0 to 50% (Buffer A: 0.05 % Trifluoroacetic acid (TFA) and Buffer B: 50% acetonitrile; 0.05 % TFA) and eluate monitored at 206nm. Some peaks from the chromatograms of peptidoglycan from *M. smegmatis* and *M. smegmatis* Δ *namH* collected under the same conditions were sent to mass spectrometry (Pasteur Institute) (data not shown). The corresponding peaks in *M. tuberculosis* were identified with their corresponding HPLC retention times which were exactly identical to the retention time from *M. smegmatis* muropeptides for which identity was determined.

Reference

Hayashi K: **A rapid determination of sodium dodecyl sulfate with methylene blue.** *Anal Biochem* 1975, **67**:503-506.

Appendix II

Age and Gender of Nod2^{-/-} and Nod2^{+/+} mice used in second aerosol infection

Due to the inherent variability of age/gender in the Nod2^{-/-} mice in our facility, for aerosol infections mice were matched with Nod2^{+/+} littermates of approximately the same age/gender. Younger mice were used for later time points in order to increase chances of survival for long-term studies. Males were also preferentially chosen for early time points because they occupy more cages in the facility, since fighting may occur if foreign males are combined. Genders are designated ‘M’ for male and ‘F’ for female, while the approximate age, in weeks, is in brackets. Mice were infected with either H37Rv Pasteur *wild-type* (WT), the *namH* knockout strain (knockout) or the complement and sacrificed at the designated time points post-infection.

Mice/time point	WT	Complement	Knockout
NOD2 3 wks	3M (20) & 2M (16)	n/a	4M (16) & 1M (20)
NOD2 6 wks	5F (12)	n/a	5F (12)
NOD2 12 wks	2F (16) & 3M (12)	n/a	5M (12)
C57Bl/6 1 day	5F (8)	5F (8)	5F (8)
C57Bl/6 1 wk	5M (12)	5M (16)	2M (12) & 3M (16)
C57Bl/6 2 wks	5M (12)	5M (16)	5M (12)
C57Bl/6 3 wks	5M (16)	5M (16)	5M (16)
C57Bl/6 6 wks	5F (16)	5F (16)	5F (16)
C57Bl/6 12 wks	5F (12)	5F (9)	2F (12) & 3F (16)
C57Bl/6 18 wks	5F (9)	5F (9)	5F (9)